Neural Networks 102 (2018) 120–137

Contents lists available at ScienceDirect

Neural Networks

journal homepage: www.elsevier.com/locate/neunet

Review

Connectivity inference from neural recording data: Challenges, mathematical bases and research directions

Ildefons Magrans de Abril [a,c,*], Junichiro Yoshimoto [b], Kenji Doya [a]

[a] Okinawa Institute of Science and Technology, Graduate University, Japan
[b] Nara Advanced Institute of Science and Technology, Japan
[c] ARAYA, Inc., Tokyo, Japan

ARTICLE INFO

Article history:
Received 16 September 2016
Received in revised form 23 February 2018
Accepted 26 February 2018
Available online 10 March 2018

Keywords:
Connectivity inference
Functional connectivity
Effective connectivity
Multi-electrode recording
Calcium fluorescence imaging

ABSTRACT

This article presents a review of computational methods for connectivity inference from neural activity data derived from multi-electrode recordings or fluorescence imaging. We first identify biophysical and technical challenges in connectivity inference along the data processing pipeline. We then review connectivity inference methods based on two major mathematical foundations, namely, descriptive model-free approaches and generative model-based approaches. We investigate representative studies in both categories and clarify which challenges have been addressed by which method. We further identify critical open issues and possible research directions.

Contents

* Corresponding author at: Okinawa Institute of Science and Technology, Graduate University, Japan.
E-mail address: ildefons.magrans@gmail.com (I. Magrans de Abril).

https://doi.org/10.1016/j.neunet.2018.02.016

1. Introduction

Understanding operational principles of neural circuits is a major goal of recent international brain science programs, such as the BRAIN Initiative in the U.S. (Insel, Landis, & Collins, 2013; Martin & Chun, 2016), the Human Brain Project in the E.U. (Amunts et al., 2016; Markram 2012), and the Brain/MINDS program in Japan (Okano & Mitra, 2015; Okano et al., 2016). A common emphasis in these programs is utilization of high-throughput, systematic data acquisition and advanced computational technologies. The aim of this paper is to present a systematic review of computational methods for inferring neural connectivity from high-dimensional neural activity recording data, such as multiple electrode arrays and calcium fluorescence imaging.

Why do we need to infer neural connectivity? High-dimensional neural recording data tell us a lot about information representation in the brain through correlation or decoding analyses with relevant sensory, motor, or cognitive signals. However, in order to understand operational principles of the brain, it is important to identify the circuit mechanisms that encode and transform information, such as extraction of sensory features and production of motor action patterns (Churchland & Sejnowski, 1992). Knowing the wiring diagram of neuronal circuits is critical to explain how such representations are produced, predicting how the network would behave in a novel situation, and extracting the brain's algorithms for technical applications (Sporns, Tononi, & Kötter, 2005).

The network of the brain can be analyzed at various spatial scales (Gerstner, Kistler, Naud, & Paninski, 2014). At the macroscopic level, there are more than a hundred anatomical brain areas and connection structure across those areas give us an understanding of the overall processing architecture of the brain. At the mesoscopic level, connections of neurons within each local area, as well as their projections to other areas, are characterized in order to understand computational mechanisms of neural circuits. At the microscopic level, locations and features of synapses on dendritic arbors of each neuron are analyzed to understand operational mechanisms of single neurons.

This review focuses on the mesoscopic level, inferring connections between neurons in local circuits on the basis of neural activity recording data from multi-electrode recordings or fluorescence imaging. Connectivity inference from anatomical data, such as diffusion MRI at the macroscopic level, tracer injection at the mesoscopic level, and serial electron microscopy data at the microscopic data, are beyond the scope of this review. Some methods, especially those of model-free approaches, may also be applicable to connectivity inference from functional MRI data at the macroscopic level.

This paper presents an overview of challenges in network inference and different mathematical approaches to address those challenges. We first review the data processing pipeline of connectivity analysis and identify both biophysical and computational difficulties. From mathematical viewpoint, we classify connectivity inference methods broadly into descriptive, model-free approaches and generative, model-based approaches and explain representative methods in each category. We then examine which

methods offer solutions for specific challenges and identify open issues and important research directions.

There have been several recent reviews of specific mathematical frameworks in network connectivity inference, such as Bayesian approaches (Chen, 2013) and the maximum entropy method (Roudi, Dunn, & Hertz, 2015; Yeh et al., 2010). Some reviews focus on macroscopic connectivity analysis using MRI (Friston, 2011; Lang, Tomé, Keck, Górriz-Sáez, & Puntonet, 2012; Sporns, 2012, 2013). Reports from the First Neural Connectomics Challenge (http://connectomics.chalearn.org) review top-ranked methods for connectivity inference from calcium imaging data (Guyon et al., 2014; Orlandi, Ray etal., 2014).

It is important to distinguish several types of connectivity that have been addressed previously (Aertsen, Gerstein, Habib, & Palm, 1989; Friston, 2011; Valdes-Sosa, Roebroeck, Daunizeau, & Friston, 2011). *Functional* connectivity (FC) is defined as statistical dependence among measurements of neuronal activity. It can be computed using correlation or other model-free methods (see Section 4). *Effective* connectivity (EC) characterizes the direct influence exercised between neuron pairs after discounting any indirect effects. EC is usually computed by optimizing parameters of a model that is assumed to have generated the observed data (see Section 5). *Anatomical* connectivity signifies existence of actual synapses, either excitatory or inhibitory. Even if there is an anatomical connection between neurons, it may not be detected when, for example, the source neuron is inactive or the recipient neuron is unresponsive due to strong inhibition by other neurons. Detection of functional or effective connectivity does not warrant the existence of anatomical connectivity. An example would be a false positive connection inferred between two neurons that receive common inputs from a third neuron.

Neural connectivity can be described at different levels of detail: existence, direction, sign, magnitude, and temporal dynamics. The level of description that is most reliable and useful depends on constraints on instrumentation and the amount of data available. One aim of this paper is to clarify how those constraints affect the choice of inference and validation methods for a given application.

Although it is beyond the scope of this review, graph theoretical analysis of the inferred network can play a key role in understanding the interplay between the brain structure and its function (Bullmore & Sporns, 2009). Such graph theoretic characterization includes clustering and connectivity degree distribution (Bonifazi et al., 2009; Shimono & Beggs, 2014; Yu, Huang, Singer, & Nikolić, 2008). These abstract metrics facilitate comparison of the structure of diverse neural populations. For example, Hu et al., (2016) proposed a method to relate the network statistics of connectivity of linear point processes or Hawkes models (see Section 5.1.6) to its function.

2. Data processing pipeline

This section presents a generic data processing pipeline, starting with data acquisition and continuing with data pre-processing, network inference, post-processing, and validation of results. Fig. 1 shows the overall view of the experimental setup.

2.1. Data acquisition

Multiple electrodes and fluorescence imaging are two major methods for making high-dimensional measurements of single neuronal activities.

2.1.1. Multiple electrode recording

For *in vivo* multiple neural recordings, the most commonly used device is the so-called "tetrode", a bundle of four wire electrodes. By implanting tens of tetrodes and applying a spike sorting method, it is possible to record hundreds of neurons simultaneously (Buzsaki, 2004; Jog et al., 2002). Linear or matrix arrays of electrodes, often using semiconductor technologies, are also used for recording hundreds of neurons near the cortical surface (Fujishiro, Kaneko, Kawashima, Ishida, & Kawano, 2014). For brain tissue slices and cultures, electrode grids patterned on a plate enable recording of hundreds of neural activities (Fujisawa, Amarasingham, Harrison, & Buzsáki, 2008; Shimono & Beggs, 2014). In such *in vitro* experiments, it is also possible to use intracellular glass electrodes to record sub-threshold membrane potentials of selected neurons in a population (Brette & Destexhe, 2012, chap. 3).

2.1.2. Optical imaging

Optical imaging allows activity data gathering from hundreds to thousands of neurons simultaneously, using voltage sensitive dyes (VSDs) or genetically encoded calcium indicators (GECIs). Chemical VSDs offer high temporal resolution, but lack the cell type-specificity that GECIs offer. However, genetically encoded voltage indicators (GEVIs) are in active development (Yang & St-Pierre, 2016). Recently GECIs have become increasingly popular because they can be expressed under the control of cell-type specific promoters (Looger & Griesbeck, 2011). The weaknesses of GECIs have been their slow temporal response and low sensitivity, but recent GECIs have begun to achieve time constants on the order of ten milliseconds, making detection of single spikes feasiible (Pnevmatikakis et al., 2016).

Fast CCD cameras and confocal or two-photon laser scanning microscopes are commonly used with GECIs. CCD cameras enable simultaneous imaging of all neurons in the focal plane, allowing recording of as many as a thousand frames per second, but measurements are limited to neurons near the surface of the tissue. Two-photon microscopes use infrared light, which is less subject to refraction and which excites fluorescent molecules only at the focal point, allowing recording of neurons several hundreds of microns beneath the surface (Dombeck, Graziano, & Tank, 2009; Lütcke & Helmchen, 2011). Most recently, head-mount miniature microscopes using gradient index (GRIN) rod lenses have allowed access to deep neural structures, such as the hippocampus of awake behaving animals (Ziv et al., 2013).

2.2. Pre-processing

Pre-processing steps depend on recording methods and specific input requirements of the network inference method.

In multiple electrode recording, each electrode can receive signals from multiple neurons and signals from the same neuron can be detected by multiple electrodes. Spike sorting algorithms are used to identify spikes from each neuron by applying principal component analysis, independent component analysis, and any biophysical knowledge of spike shapes and intervals (Mahmud, Pulizzi, Vasilaki, & Giugliano, 2015; Shimono & Beggs, 2014).

The task in optically imaged data pre-processing is to transform an image sequence into a multi-dimensional time-series of neural activities. Pre-processing steps for optical imaging are: (i) image segmentation to identify regions corresponding to each neuron, (ii) extraction of the fluorescence trace for each neuron and (iii) spike inference (Pnevmatikakis et al., 2016). These pre-processing operations have to deal with light scattering, motion artifacts, and slow fluorescence changes with respect to the underlying membrane potential.

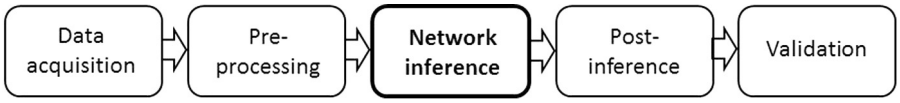

Fig. 1. Generic data processing pipeline, starting with data acquisition and continuing with data pre-processing, network inference, post-processing, and validation of results.

2.3. Connectivity inference

Connectivity inference methods can be largely classified into two classes. Descriptive model-free methods are based on descriptive statistics without assuming any particular process that generated the data. On the other hand, generative model-based methods assume a certain mathematical model that generates the data and infer parameters and structure of the model. We will explain those methods in detail in subsequent sections.

Most connectivity inference methods require time-series of spikes from each neuron in the population. In some studies, spike inference and connectivity inference are performed using an integrated optimization algorithm directly from time-series of fluorescence (Mishchenko, Vogelstein, & Paninski, 2011). Some other studies use fluorescence signals directly for model-free analysis of connectivity without an explicit spike inference mechanism (Veeriah, Durvasula, & Qi, 2015).

2.4. Post-processing

After the connectivity matrix is obtained by applying any of the connectivity inference methods, it is often useful to perform post-processing to achieve a biologically realistic result. For example, inference methods that consider only simultaneous activities yield only symmetric connectivity matrices. A heuristic method to determine the direction is to use the average temporal order of activations of two neurons (Sutera et al., 2014). Another issue is that inferred connectivity can be a mix of direct causal effects between neuron pairs and indirect effects through other neurons. One way to address this problem is to use matrix deconvolution (Barzel & Barabási, 2013; Feizi, Marbach, Médard, & Kellis, 2013; Magrans & Nowe, 2014), as described in Section 6.1.2.

Furthermore, employment of a network inference method depends on the choice of parameters. It is possible to improve both robustness and accuracy of the connectivity matrix by combining several matrices computed using different parameters and/or different inference methods (Magrans & Nowe, 2014; Sutera et al., 2014).

2.5. Validation

In order to validate the connectivity inference method itself, use of synthetic data from a network model with a known connection matrix is the first step. For estimating connectivity of real biological neural networks, validation is more challenging, as anatomical or physiological verification of all pair-wise synaptic connectivity is extremely laborious.

2.5.1. Synthetic data

The strength of synthetic data for validation is that we have all information about simulated connectivity and other biophysical parameters of the model. Therefore, we can use standard error metrics to measure the similarity between the inferred connectivity matrix and the one used for data generation.

When the final objective is to infer connection weights, one difficulty with many methods is that they deliver estimated connectivity values with different scales. The relative mean squared error

$$relative\ MSE = \frac{min_\alpha \sum_{ij} |W_{ij} - \alpha \hat{W}_{ij}|^2}{\sum_{ij} |W_{ij}|^2}, \quad (1)$$

where $\hat{W}_{ij}$ is the estimate of W_{ij}, can alleviate the scaling problem (Fletcher & Rangan, 2014).

If the objective is to infer the graphical structure of the network, what matters is the binary existence/nonexistence of connections. The Area Under the Curve of the Receiver–Operator Characteristic (AUROC) is a popular performance metric used in such a case (Garofalo, Nieus, Massobrio, & Martinoia, 2009; Guyon et al., 2014; Stetter, Battaglia, Soriano, & Geisel, 2012). The ROC Curve describes the relationship between the False Positive (FP) Rate ($\frac{FP}{FP+TN}$) or Fall-out and the True Positive (TP) Rate ($\frac{TP}{TP+FN}$) or Recall at different thresholds. The perfect classifier has an AUROC of 1, while a random classifier has an AUROC of 0.5. However, this metric may overestimate performance in highly biased datasets (Schrynemackers, Küffner, & Geurts, 2013). The Area under the Precision Recall Curve (AUPRC) was proposed as an alternative measure to improve validation accuracy of sparsely connected neural networks (Orlandi et al., 2014; Sutera et al., 2014). Specifically, it is the area below the curve that describes the relationship between the Precision ($\frac{TP}{TP+FP}$) versus the Recall ($\frac{TP}{TP+FN}$) at different thresholds.

In order to find the best trade-off between *TP*s and *FP*s, Garofalo et al. (2009) defined the Positive Precision Curve (PPC), which describes the relationship between the True False Sum ($TFS = TP + FP$) and the True False Ratio ($TFR = \frac{TP-FP}{TFS+TN}$). The peak of this curve can be used to extract a binary connectivity map from a weight matrix inferred by a network inference method. To assess the required recording duration and bin size to achieve a desired reconstruction performance, Ito et al. (2011) proposed the use of the curves of the TPR at a fixed FPR as a function of different recording durations and bin sizes.

2.5.2. Real data

In real neural recording, although the ground truth of connectivity is not generally available, we can assess quality of inferred connections using statistical significance testing and cross validation. Significance testing is used to accept or reject the null hypothesis (H_0) that a connection between two neurons does not exist (Lizier, 2014). To approximate H_0, we can run our network inference method on many surrogate time-series created by perturbing the training time-series such that it destroys the connectivity information (Fujisawa et al., 2008; Lizier, Heinzle, Horstmann, Haynes, & Prokopenko, 2011; Oba, Nakae, Ikegaya, Aki, Yoshimoto, & Ishii, 2016; Shimono & Beggs, 2014). Then, the test itself consists of computing the probability that the inferred connectivity value is generated uniquely by chance. However, sometimes an accept/reject test is not enough, as for instance, when we wish to infer a weighted connectivity matrix or parameters like the synaptic delay or a time constant from a biophysical model.

Model structures and/or parameter sets in a certain class can be compared using relative quality measures like the likelihood ratio and other criteria that penalize larger complexity models like the Akaike Information Criterion (AIC) and the Bayesian Information Criterion (BIC) (Aho, Derryberry, & Peterson, 2014).

An alternative strategy is cross validation, in which the inferred model is tested against a separate test data set that was not used for model inference. A standard method in probabilistic model-based methods is to compute a normalized likelihood of the model for a test data set (Gerwinn, Macke, & Bethge, 2010). In addition, comparison of any statistical features, such as average firing rates

and spike-train statistics of the sample data produced from the inferred model and the real data is helpful in validating the inferred model (Pillow, Paninski, Uzzell, Simoncelli, & Chichilnisky, 2005). When a certain graph-theoretic feature of the network is known, for example, by previous anatomical studies, comparison of such features, such as the node degree distribution, can be a helpful way of validation (Bullmore & Sporns, 2009).

3. Challenges

This section summarizes two types of challenges in connectivity inference: biophysical and technical. We first describe complexities arising from biophysical properties of neurons and synapses, and then from technical difficulties due to constraints in instrumentation and computation.

3.1. Biophysical challenges

Apparent connectivity: As mentioned in the Introduction, functional connectivity (FC) and effective connectivity (EC) may not be due to direct synaptic connectivity. A typical example is a common input that activates two or more neurons simultaneously. In such a case, functional connectivity can be inferred between the recipient neurons even if there is no direct connection between them. Other cases are a common input with different time delays or an indirect connection through a third neuron, which can activate two neurons in sequence. In this case, effective connectivity can be inferred even if there is no direct synaptic connection between them.

Directionality: Methods based on simple correlation cannot detect the direction of the causal or temporal relationship. Even when the temporal order of activities is considered, if time resolution of the measurement or analysis is coarse, ordered activation can appear as simultaneous activation, making it difficult to determine directionality.

Cellular diversity: Many neurons show intrinsic refractoriness such that spike frequency gradually drops even with a constant level of input. Some neurons also show a burst property such that once excited above a threshold, they keep spiking even without excitatory inputs. In such cases, it is not straightforward to discriminate whether a change in the activity of a neuron is due to some network dynamic or the neuron's intrinsic properties (Gerstner et al., 2014: chap. 1). Such refractoriness or burstiness can be categorized as inhibitory or excitatory self-connection, but whether it actually results from self-connecting synapses (autapse) (Bekkers, 2009) must be carefully interpreted. Even in a local circuit, there are many different types of neurons with a large diversity of biophysical parameters (Kandel, Schwartz, Jessell, et al., 2000a, chap. 4). Thus a simple assumption of uniform cellular properties may not be valid.

Synaptic diversity: Diversity also applies to connectivity because underlying synapses can have complex and diverse characteristics (e.g. excitatory/inhibitory, facilitatory/depressive, delays, etc.) (Kandel, Schwartz, Jessell, et al., 2000b, chap. 8). Understanding how a given effective network emerges may require the inference of many additional parameters beyond a simple weight matrix.

Non-stationarity: Synaptic weights are subject to both short-term (from tens of milliseconds to few minutes) and long-term changes (from minutes to hours) (Gerstner et al., 2014: chap. 19). Physiological states of neurons can also drift over time, especially during experimental manipulations, as in slice preparations, with electrodes inserted, or with exposure to light. *In vitro* cultured neural networks often manifest switching between states of low- and high-firing rates. When using fluorescence imaging, the high firing state can cause erroneous connectivity inference because the low temporal resolution makes it difficult to discriminate between direct and indirect effects (Stetter et al., 2012).

3.2. Technical challenges

Noise: Every instrument is subject to noise. Electrodes can pick up both biophysical (e.g. thermal noise) and anthropogenic noise (e.g. electromagnetic interference from power lines) (Van Drongelen, 2006). Optical imaging is susceptible to light scattering artifacts, and motion artifacts in awake subjects with *in vivo* imaging. Even though motion correction programs can track shifts of neurons within an image, movement of cells out of the focal plane is difficult to compensate.

Time/space resolution: Multi-electrode recording can monitor activities of a few hundred neurons with sampling rates on the order of 10 kHz (Shimono & Beggs, 2014). Fluorescence imaging can work with a trade-off of space and time, ranging from few hundred neurons recorded at 100 Hz to a hundred thousand neurons, or 80% of a zebra fish brain, at a rate of 0.8 Hz (Ahrens, Orger, Robson, Li, & Keller, 2013). The poor temporal resolution of fluorescence imaging has the undesirable feature of mixing indirect causal effects with real direct connectivity effects.

Hidden neurons/External inputs: Even though recent advances in two-photon imaging have enabled us to capture thousands of neurons at one time (Ahrens et al., 2012), it is still difficult to simultaneously record the activity of every single neuron in a circuit. Neglecting hidden neurons can lead to spurious detection of connectivity between neurons connected via hidden neurons. Even though most experiments take into account sensory stimuli or motor actions in the analysis of neural activities, the brain shows various intrinsic dynamics. Unknown external inputs, especially those common to multiple neurons, can also result in a detection of spurious connections.

Prior knowledge: Prior knowledge of the anatomy and physiology of the neural network under investigation can be leveraged to enhance connectivity inference. How to incorporate prior knowledge about the composition of neuron types in a population (Shimono & Beggs, 2014; Sohn, Choi, Ahn, Lee, & Jeong, 2011) or connection probabilities between different types of neurons (White, Southgate, Thomson, & Brenner, 1986) to constrain the solution space is an important issue in connectivity inference. Additional data, such as the local field potential (Destexhe & Bedard, 2013), can also facilitate understanding of non-stationary behaviors at the microcircuit level.

Scalability: As the number of neurons measured simultaneously grows from hundreds to thousands, the number of potential connections grows from tens of thousands to millions. Therefore, inference methods need to be designed to maximize computational efficiency and to minimize the cost of parallelized implementations (Gerstner et al., 2014: chap. 10).

4. Model-free methods

We first review *model-free* methods, which do not assume any mechanism to generate the observed data. These methods tend to be simpler than model-based methods, but they are not able to generate activity data for model validation or prediction. We will review model-free methods in two categories. The first is based on descriptive statistics and the second on information theoretic concepts. Tables 1.1 and 1.2 summarize the major model-free methods and examples that use those methods.

Table 1.1
Summary of model-free connectivity inference methods, Descriptive Statistics (4.1).

Method	Principle	Examples of application	Features
Correlation (4.1.1)	Linear relationship	Magrans and Nowe (2014): simulation data that assume calcium imaging Fujisawa et al. (2008): Multi-electrode recordings from medial prefrontal cortex of rats Cohen and Kohn (2011)	• Acausal indicator • Does not discriminate direct/indirect effects • Low computational cost
Cross-correlation (4.1.2)	Linear relationship with time shift	Garofalo et al. (2009): ROC and PPC curves for CC below JE and TE Ito et al. (2011): ROC curve for CC below TE variants curves Knox (1981) Garofalo et al. (2009): simulation data and multi-electrode recordings from in vitro cultured cortical neurons Ito et al. (2011): simulation data	• Causal indicator • Takes into account the spike train history • Low computational cost
Partial-correlation (4.1.3)	Linear relationship excluding the effect from other neurons	Sutera et al. (2014): simulation data that assume calcium imaging	• Acausal indicator • Discriminates direct/indirect effects • Solution based on PC won First Neural Connectomics Challenge

Table 1.2
Summary of model-free connectivity inference methods, Information Theoretic (4.2) and Supervised Learning (4.3, 6.1.3).

Method	Principle	Examples of application	Features
Mutual information (4.2.1)	Statistical dependence	Garofalo et al. (2009): ROC and PPC curves for MI below TE, JE and CC curves Garofalo et al. (2009): simulation data and multi-electrode recordings from in vitro cultured cortical neurons	• Acausal indicator • Does not discriminate direct/indirect effects • Does not discriminate between excitatory and inhibitory connections
Joint entropy (4.2.2)	Entropy of cross-inter-spike-intervals	Garofalo et al. (2009): ROC and PPC curves for JE below TE and above MI and CC curves Garofalo et al. (2009): simulation data and multi-electrode recordings from in vitro cultured cortical neurons	• Acausal indicator • Does not discriminate direct/indirect effects • Does not discriminate between excitatory and inhibitory connections
Transfer entropy (4.2.3)	Gain in past-future mutual information when the activity of another neuron is considered	Garofalo et al. (2009): ROC and PPC curves for TE above the rest (JE, MI and CC curves) Schreiber (2000) Garofalo et al. (2009): simulation data and multi-electrode recordings from in vitro cultured cortical neurons Shimono and Beggs (2014): multi-electrode recordings from from slice cultures of rodent somatosensory cortex	• Causal indicator • Does not discriminate direct/indirect effects • Does not discriminate between excitatory and inhibitory connections. However, it is possible to perform a subsequent analysis of the correlation or conditional distribution to infer if it is excitatory or inhibitory • Takes into account the spike train history
Delayed transfer entropy (4.2.4)	Transfer entropy with delayed source signal	Ito et al. (2011): ROC curve and TPR at constant FPR better than TE and below HOTE Ito et al. (2011): simulation data	• Same as transfer entropy
High order transfer entropy (4.2.5)	Transfer entropy with multiple time steps of activities	Ito et al. (2011): ROC curve and TPR at constant FPR better than TE and DTE Ito et al. (2011): simulation data	• Same as transfer entropy
Generalized transfer entropy (4.2.6)	Transfer entropy with present source activity, after removing high activity periods	Orlandi, Stetter et al., (2014); Stetter et al. (2012): ROC curve for GTE above TE curve Orlandi, Stetter et al. (2014); Stetter et al. (2012): simulation data that assume calcium imaging and data recorded using calcium imaging from in vitro networks derived from cortical neurons	• The use of information from the same time bin for both neurons enhances reconstruction performance when the data source has a low sampling rate (e.g. calcium imaging) • It copes well with synchronized bursting episodes
Convolutional neural network (6.1.3)	Probability of connection generalized from training data	Romaszko (2014); Veeriah et al. (2015): simulation data that assume calcium imaging	• It assumes the ground truth connectivity labels of a training data set that has similar properties as the network that we want to reconstruct

We denote the neural activity data set as

$$D = \{x_i(t) | i = 1, \ldots, P;\ t = 1, \ldots, T\},$$

where $x_i(t)$ is the activity of neuron i at the tth time point. $x_i(t)$ may be continuous, for instance, when values are raw data obtained from multiple electrodes or fluorescence imaging, or it may be binary when data are transformed into a spike train by a spike-sorting algorithm.

4.1. Descriptive statistics

This method class utilizes statistical measures to capture the degree of connection between neurons from a sample of activities from a neural population.

4.1.1. Correlation

Correlation indicates the strength of the linear relationship between two random variables that represent two neurons. The

most commonly used measure of correlation between activities x_i and x_j of two neurons i and j is the Pearson correlation coefficient defined as:

$$\rho_{ij} = \frac{\Sigma_{ij}}{\sqrt{\Sigma_{ii}\Sigma_{jj}}}, \tag{2}$$

where $\Sigma_{ij} = \frac{1}{T}\sum_{t=1}^{T}(x_i(t) - \mu_i)(x_j(t) - \mu_j)$ is the covariance and $\mu_i = \frac{1}{T}\sum_{t=1}^{T}x_i(t)$ is the mean activity.

When we use correlation ρ_{ij} to perform network inference of neuronal circuits, we are measuring the rate of co-occurring spikes of neurons i and j (Cohen & Kohn, 2011) and this rate is interpreted as the functional connectivity strength. While Pearson correlation is computationally least costly, it has a number of drawbacks. It is not able to indicate the causal direction and it cannot distinguish direct connections from indirect ones. It is also not suited to deal with external inputs. Despite such limitations, a winning solution of the First Neural Connectomics Challenge used correlation as a key component in a more complex method (see Section 6.1.2).

4.1.2. Cross correlation

Cross correlation (CC) indicates the strength of the delayed linear relationship between two neurons i and j. Knox (1981) defines CC as "the probability of observing a spike in one train x_j at time $t + \tau$, given that there was a spike in a second train x_i at time t". Ito et al. (2011) remark that, despite the extensive literature, there is no standard definition, and they discuss the two most popular ones:

$$\rho_{i\to j}(\tau) = \frac{1}{T-1}\sum_{t=1}^{T}\frac{(x_i(t) - \mu_i)(x_j(t+\tau) - \mu_j)}{\sigma_i\sigma_j} \tag{3}$$

where the parameter τ defines the delay of neuron j with respect to neuron i, and μ and σ are the sample average and standard deviation, respectively.

The second CC definition uses the total number of spikes instead of the averages and standard deviations:

$$\rho_{i\to j}(\tau) = \sum_{t=1}^{T}\frac{x_i(t)x_j(t+\tau)}{\sqrt{n_i n_j}}, \tag{4}$$

where n_i and n_j are the total number of spikes from neuron i and j respectively. Both cross-correlation definitions tend to be equivalent when μ_i and μ_j approach 0.

CC is a causal indicator that is able to indicate the direction of the connection. Inference performance of the connection direction depends upon the instrumentation sampling rate and the choice of time delay τ. Despite being able to detect the direction of connectivity, CC has the same limitations as correlation in dealing with indirect connections and external inputs.

We should also note that the optimal parameter τ to detect a connection can be different for each connection. A measure to address this issue is the Coincidence Index (CI), which combines several CCs computed at different τs:

$$CI_{i\to j} = \frac{\sum_{\tau=0}^{r}\rho_{i\to j}(\tau)}{\sum_{\tau=0}^{T}\rho_{i\to j}(\tau)}, \tag{5}$$

where r specifies the interval of cross-correlation delays, called the coincidence interval. A large CI indicates a larger reproducibility of correlated spike timing (Chiappalone, Vato, Berdondini, Koudelka-Hep, & Martinoia, 2007; Shimono & Beggs, 2014; Tateno & Jimbo, 1999).

Garofalo et al. (2009) evaluated the network inference performance of several model-free methods using data from simulated neuronal networks with only excitatory synapses and including both excitatory and inhibitory connections. According to both ROC and PPC criteria, CC demonstrated a performance just below transfer entropy (TE, see Section 4.2.3) in the fully excitatory setting, and below TE and joint entropy (JE, see Section 4.2.2) when inhibitory connections were also included. Ito et al. (2011) evaluated the inference performance of the two CC variants discussed in this section and several transfer entropy variants (see Sections 4.2.4, 4.2.5 and 4.2.6) using data from simulated neuronal networks with both excitatory and inhibitory connections. According to the ROC criterion, both CC variants showed a performance inferior to all variants of transfer entropy.

4.1.3. Partial correlation

Let $R = [R_{ij}]$ be an inverse of a covariance matrix Σ of which the (i, j)th component is Σ_{ij}. The definition of partial correlation (PC) between activities of neurons i and j is:

$$PC_{ij} = -\frac{R_{ij}}{\sqrt{R_{ii}R_{jj}}}. \tag{6}$$

The most salient difference between PC and other methods described in this section is that PC takes into account the activities of all neurons in the population to compute a connectivity indicator between each neuron pair. An important property of PC is that, assuming that $x(t) = (x_1(t), \ldots, x_P(t))$ is normally distributed, then PC_{ij} is 0 if and only if neurons i and j are independent given all the rest. Therefore, PC can be used to distinguish a direct effect from an indirect one. Despite this multivariate feature, PC shares the same limitations as correlation and CC in dealing with external inputs, with the additional computational complexity required to invert the covariance matrix. The first prize solution of the First Neural Connectomics Challenge, discussed in Section 6.1.1, is a good example of how to use PC for network inference (Sutera et al., 2014).

4.2. Information theoretic methods

Information theory is a mathematical discipline initiated by Shannon to characterize the limits of information management, including transmission, compression and processing (Shannon, 1948). This section presents the application of several information theory measures to the inference of neural microcircuits.

4.2.1. Mutual information

Mutual information (MI) is a measure of the statistical dependence between stochastic variables. MI of activities x_i and x_j of two neurons is mathematically defined as:

$$MI_{i,j} = \sum_{i,j}P(x_i, x_j)\log\frac{P(x_i, x_j)}{P(x_i)P(x_j)}. \tag{7}$$

This indicator is symmetric; therefore it is unable to identify the direction of the connection. It cannot discriminate direct effects from indirect effects. One way to overcome the directionality limitation is to introduce a delay as in CC, and to consider multiple delays as in CI (Garofalo et al., 2009).

In a comparative study by Garofalo et al. (2009) using data from simulated neuronal networks, MI delivered the performance below TE, JE and CC, according to both ROC and PPC criteria.

4.2.2. Joint entropy

Joint entropy (JE) is a bi-variate causal measure between the activity of two neurons, testing whether neuron i is a cause of the activity in neuron j. For each reference spike in x_i, the closest future spike on x_j is identified and the cross-inter-spike-interval is computed as $cISI = t_{x_i} - t_{x_j}$, where tx_i and t_{x_j} are the time of

successive spikes of neuron i and j, respectively. Then JE is defined as the entropy of the cISI distribution:

$$JE_{i\to j} = -\sum_k P(cISI_k)\log_2 P(cISI_k), \tag{8}$$

where k indexes the level of cISI. If neurons i and j are strongly connected, then JE is expected to be close to 0 as the cISI distribution becomes sharp.

In a comparison by Garofalo et al. (2009), JE showed the worst performance below TE, CC and MI in a fully excitatory setting, but the second best performance below TE when inhibitory connections were also included.

4.2.3. Transfer entropy

Transfer entropy (TE) is a causal indicator defined between the activity of two neurons i and j. The definition of TE was originally formulated as the Kullback–Leibler divergence between the distributions of the neural activity of target neuron j conditioned by its previous activities alone versus conditioned also by previous activities of source neuron i (Schreiber, 2000):

$$\begin{aligned} &TE_{i\to j} \\ &= \sum P(x_j(t), x_j(t-1), \ldots, x_j(t-k), x_i(t-1), \ldots, x_i(t-l)) \\ &\log_2 \frac{P(x_j(t)|x_j(t-1), \ldots, x_j(t-k), x_i(t-1), \ldots, x_i(t-l))}{P(x_j(t)|x_j(t-1), \ldots, x_j(t-k))} \end{aligned} \tag{9}$$

TE can also be defined as the conditional mutual information between the future activity of target neuron j and past activity of source neuron i conditioned by past activity of target neuron j, which can also be expressed as the amount of uncertainty reduced in the future activity of neuron j knowing the past activity of i given past activity of j:

$$\begin{aligned} &TE_{i\to j} \\ &= MI(x_j(t), (x_i(t-1), \ldots, x_i(t-l))|(x_j(t-1), \ldots, x_j(t-k))) \\ &= H(x_j(t)|(x_j(t-1), \ldots, x_j(t-k))) \\ &\quad - H(x_j(t)|(x_j(t-1), \ldots, x_j(t-k), x_i(t-1), \ldots, x_i(t-l))) \end{aligned} \tag{10}$$

From this second definition, we can see that TE is a positive measure that takes a low value when the past activity of neuron i does not convey information about the future activity of neuron j.

TE is equivalent to Granger causality for Gaussian variables (Barnett, Barrett, & Seth, 2009). A nice feature of TE is that it can detect non-linear relationships (Stetter et al., 2012). Although TE does not identify whether the connection is excitatory or inhibitory, the polarity of connection can be tested separately by recording (real data) or simulating the same network with the inhibitory connections pharmacologically blocked (Orlandi, Stetter et al., 2014; Stetter et al., 2012). The performance of TE in discriminating the causal direction depends whether the sampling rate is faster than the network dynamics (Fujisawa et al., 2008; Shimono & Beggs, 2014).

In practice, the parameters k and l in Eq. (9) are set to 1 (e.g., Garofalo et al. (2009)), so that we only have to consider a small number of patterns (i.e. $2^3 = 8$ for binary data). While increasing k and l can allow detection of delayed effects of a connection, it requires larger amount of data to have reliable estimates of the probability distribution to compute the entropies.

Before the First Neural Connectomics Challenge, TE was arguably the most successful model-free method (Garofalo et al., 2009; Stetter et al., 2012). This success encouraged a number of variants as follows (Ito et al., 2011; Orlandi, Stetter, et al., 2014; Stetter et al., 2012).

4.2.4. Delayed transfer entropy (DTE)

A limitation of TE using $k = l = 1$ is that it assumes a constant one-time bin delay between the action potential in neuron i and the post-synaptic action potential of neuron j, which is not a realistic assumption. A suboptimal way to deal with this problem is to create longer time bins at the cost of losing detailed temporal information. Instead, delayed TE (DTE) was proposed to measure TE at a user-defined time delay d (Ito et al., 2011). Compared to the original definition, instead of $x_i(t-1), \ldots, x_i(t-l)$ in Eq. (9), they suggest using a delayed signal $x_i(t-d), \ldots, x_i(t-d-l+1)$. Shimono and Beggs (2014) improve reconstruction performance by identifying the delay parameter for each individual connection using the coincidence index (Eq. (5)).

4.2.5. High order transfer entropy (HOTE)

Ito et al. (2011) considered how to increase k and l to take into account longer spike train history, while avoiding negative effects of the increase in the possible patterns (2^{k+l+1}). The additional parameters d in DTE and k and l in HOTE give multiple measures for each neuron pair. They evaluated the reconstruction performance by the peak value and the coincidence index (Eq. (5)) of DTE and HOTE, using a simulated network with both excitatory and inhibitory connections. $HOTE_{CI}$ and DTE_{CI} had better performance than $HOTE_{pk}$ and DTE_{pk}, which in turn were better than TE with $k = l = 1$.

4.2.6. Generalized transfer entropy (GTE)

As described in Section 3, periods of synchronized bursting convey very low connectivity information due to the simultaneous spike of a large percentage of neurons. This phenomenon is especially critical with calcium imaging recordings because of their limited temporal resolution. Generalized TE (Stetter et al., 2012) was proposed to alleviate this problem with two modifications to Eq. (9): (i) to compensate for the slow sampling rate in fluorescence imaging ($\geq$10 ms), GTE uses presynaptic activity from the same time bin $x_i(t)$ instead of the previous one $x_i(t-1)$; (ii) to discard the poor connectivity information conveyed by synchronized bursting periods, GTE restricts the computation of TE to those time bins with an overall network activity below a given user-defined threshold.

Just like TE, GTE is unable to differentiate between excitatory and inhibitory connections. Application of GTE to simulated neural networks with excitatory connections shows improved performance with respect to TE, and modified versions of CC and MI implementing the same generalization (Stetter et al., 2012). Orlandi, Stetter et al. (2014) showed that GTE is able to reconstruct inhibitory connections; however, its reconstruction performance is below its reconstruction performance of excitatory connections.

4.2.7. Information gain

Information gain (IG) is a less known causal indicator between the activity of two neurons i and j. Its definition is:

$$IG_{i\to j} = H(x_j(t)) - H(x_j(t)|x_i(t-1)), \tag{11}$$

where H is the entropy, x_i is the activity vector of the source neuron and x_j is the activity vector of the target neuron. In the case of calcium imaging, it may be convenient to employ the same strategy as with GTE, using the sample from the same time bin $x_i(t)$ instead of the previous one $x_i(t-1)$. This connectivity indicator was used as one of multiple indicators combined by one of the top solutions of the First Neural Connectomics Challenge (Czarnecki & Jozefowicz, 2014).

4.3. Supervised learning approach

Motivated by recent successes of deep neural networks in challenging pattern classification problems, a new approach has been proposed to apply convolutional neural networks (CNNs) for prediction of the existence of synaptic connectivity (Romaszko, 2014; Veeriah et al., 2015). In this approach, time-series data of spike trains or fluorescent signals of a pair or more of neurons are given as the input and a CNN is trained to classify if there is a connection between the neurons.

A natural limitation of this approach is that training requires sufficient ground truth data about the existence of connectivity. Although this approach has been successful with simulated data (Romaszko, 2014; Veeriah et al., 2015), it is hard to apply it directly to real data, for which experimental identification of synaptic connectivity is highly costly.

5. Model-based methods

Now we review *model-based* methods, in which the connectivity is estimated by explicitly modeling the data generation process. The basic paradigm of the model-based method is: (1) to assume a generative model that generates neural data, and (2) to determine model parameters to fit observed data. Table 2 summarizes the major model-based methods and examples that used those methods. We should keep in mind here that any model for this approach aims to explain the observed data, but does not consider all physiological properties of the real neural networks: The large number of factors affects structure and function of real neural systems, and it is infeasible for all of them to be considered in a single model (See more details about similarities and gaps between the model and biological reality in Ask and Reza (2016). Due to the limitation, the applicability of model-based methods is shown only empirically using simulation studies, but there is no theoretical guarantee that the estimation result are consistent with underlying connectivity. However, by reviewing model-based methods here, we will see approximation techniques to fill the gaps with a feasible number of parameters, as well as practical solutions for the connectivity estimate.

In the following, $x(t) = (x_1(t), \ldots, x_P(t))$ represents a set of P signals observed at the tth time point in a discrete time domain, where $x_i(t)$ denotes the ith neuron's activity at that time. $x_i(t)$ may be continuous when the measurement is raw data collected from calcium imaging and multiple-electrode recording, or binary when the data is transformed into a spike train by a spike-sorting algorithm. We denote a generative model $p_\theta(x)$, where θ is a parameter vector, including the connection weights.

5.1. Generative models

5.1.1. Autoregressive model

A basic example of a generative model is the *autoregressive (AR) model* mathematically expressed as

$$x_i(t) = A_{i0} + \sum_{j=1}^{P}\sum_{k=1}^{K} A_{ij}(k)x_j(t-k) + \epsilon_i(t), \quad i = 1, \ldots, P.$$

$$\epsilon_i(t) \sim \mathcal{N}(\cdot|0, \sigma_i^2) \tag{12}$$

where K is the degree of the model, $A_{ij}(k)$ is a parameter called an AR coefficient, A_{i0} is a bias term, and $\mathcal{N}(\cdot|\mu, \sigma^2)$ denotes the Gaussian distribution with mean μ and standard deviation σ (for simplicity, we assume that σ is known in this example).

By integrating two equations in Eq. (12), $x_i(t)$ can be regarded as a sample according to the following conditional distribution:

$$x_i(t) \sim \mathcal{N}\left(\mu_i(t), \sigma_i^2\right), \tag{13}$$

$$\mu_i(t) = A_{i0} + \sum_{j=1}^{P}\sum_{k=1}^{K} A_{ij}(k)x_j(t-k) \tag{14}$$

where $\theta \equiv \{A_{i0}|i = 1, \ldots, P\} \cup \{A_{ij}(k)|i, j = 1, \ldots, P; k = 1, \ldots, K\}$ is a set of parameters in this case.

After determining the parameter θ, if $A_{ij}(k)$ for all k is exactly or very close to zero, it implies that there is no direct interaction from the jth neuron to the ith neuron. In contrast, if $A_{ij}(k)$ for some k deviates enough from zero, the jth neuron x_j can directly affect the ith neuron x_i with a k time-step delay.

Even though a neuron's dynamics are usually nonlinear, for the virtue of simplicity, this method has been used in a wide range of neural data analyses, in addition to calcium imaging and multiple electrode recording (Franaszczuk et al., 1985; Harrison et al., 2003; Smith et al., 2011; Valdés-Sosa et al., 2005).

5.1.2. Generalized linear model

When $x_i(t)$ is a binary variable indicating whether a spike is generated at the tth time step, the generalized linear models (GLM) (Song et al., 2013) provide a tractable extension of the AR models. A GLM describes spike generation as a point process as

$$x_i(t) \sim \mathrm{Ber}(\cdot|\rho_i(t)) \tag{15a}$$

$$\rho_i(t) \equiv \phi\left(A_{i0} + \sum_{j=1}^{P}\sum_{k=1}^{K} A_{ij}(k)x_j(t-k)\right), \tag{15b}$$

where $\mathrm{Ber}(\cdot|p)$ denotes the Bernoulli distribution with an event probability of p. $\phi(\cdot)$ is a so-called an inverse link function, for which the exponential function $\phi(x) = \exp(x)$ or the sigmoid function $\phi(x) = (1 + \exp(-x))^{-1}$ is often used.

5.1.3. Stochastic leaky integrate-and-fire model

A stochastic leaky integrate-and-fire (LIF) model (Isomura et al., 2015; Koyama & Paninski, 2010; Paninski et al., 2004), is one of the most widely used models for analyzing the behavior of spiking neural networks (Gerstner et al., 2014). The model assumes that the subthreshold membrane potential of the ith neuron, denoted by V_i, evolves according to the following stochastic differential equation:

$$dV_i(t) = \left(-g_i V_i(t) + \sum_{j=1}^{P} I_{ij}(t)\right)dt + \sigma_i dW_i(t), \tag{16}$$

where g_i is the membrane leak conductance and $dW_i(t)$ is an increment of a Wiener process. I_{ij} is an influence from the jth neuron to the ith neuron, which is often assumed to be

$$I_{ij}(t) = \sum_{\{f:t_j^{(f)}<t\}} \kappa_{ij}(t - t_i^{(f)}), \tag{17}$$

where $\kappa_{ij}(s)$ represents the effect of the jth neuron to the ith neuron after a time delay s and $t_j^{(f)}$ is the fth spike of the jth neuron.

In the hard-threshold version (Paninski et al., 2004), whenever $V_i(t)$ goes over a threshold V_{th}, the neuron generates a spike. In the soft-threshold case (Isomura et al., 2015; Koyama & Paninski, 2010), the probability for the neuron to generate a spike in a small time interval dt is given by

$$\Pr\{\text{a spike in } [t, t+dt)\} = f(V(t))dt, \tag{18}$$

where $f(\cdot)$ is a non-negative intensity function.

Table 2
Summary of model-based connectivity inference methods.

Method	Principle	References & demonstrations (The asterisk (*) shows inclusion of applications to real data)	Features
Autoregressive models (5.1.1)	Directed linear interaction	* Harrison, Penny, and Friston (2003): human fMRI data * Franaszczuk, Blinowska, and Kowalczyk (1985): multichannel EEG time series Smith, Fall, and Sornborger (2011): simulation data that assume calcium imaging	• analytical solutions are available • not suitable for spike-train data
Generalized linear model (5.1.2)	Spike probability based on linear summation of inputs	* Song, Wang, Tu, Marmarelis, Hampson, Deadwyler, and Berger (2013): simulation data and multi-electrode recordings from hippocampal CA3 and CA1 regions of rats * Gerwinn et al. (2010): simulation data and multi-electrode recordings from salamander retinal ganglion cells	• easy but iterative optimization is required
Stochastic leaky integrate-and-fire model (5.1.3)	Stochastic spike with state resetting	Paninski, Pillow, and Simoncelli (2004): simulation data Koyama and Paninski (2010): simulation data Isomura, Ogawa, Kotani, and Jimbo (2015): simulation data	• model for a continuous time domain • a special case of generalized linear models
Network likelihood model (5.1.4)	Continuous-time model with Poisson spikes	* Okatan, Wilson, and Brown (2005): simulation data and multi-electrode recordings from hippocampal CA1 region of a rat * Kim, Putrino, Ghosh, and Brown (2011): simulation data and multi-electrode recordings from the primary motor cortex (MI) of a cat * Stevenson, Rebesco, Hatsopoulos, Haga, Miller, and Kording (2009): simulation data and multi-electrode recordings from the primary motor cortex (MI) and dorsal premotor cortex (PMd) of a monkey	• a special case of generalized linear models • instantaneous firing rates are directly considered
Calcium fluorescence model (5.1.5)		Mishchenko et al. (2011): simulation data	
Hawkes process (5.1.6)	GLM with Poisson observation	Linderman and Adams (2014) Linderman and Adams (2015): simulation data that assume calcium imaging	• The network consists of purely excitatory neurons
Dynamic Bayesian network (5.1.7)	Directed acyclic graph	Eldawlatly, Zhou, Jin, and Oweiss (2010) * Patnaik, Laxman, and Ramakrishnan (2011): simulation data and multi-electrode recordings from dissociated cortical cultures of rats	• Simulated annealing for optimizing both network structures and parameters • The computational efficiency is degraded in case of cyclic graphs • Due to the nature of Bayesian approach, the result depends on hypothetical choices of the prior distribution.
Maximum entropy model (5.1.8)	Maximum entropy under constraint by an energy function	* Tkacik, Mora, Marre, Amodei, Berry, Michael, and Bialek (2014): multi-electrode recordings from retinal ganglion cells	• Inspired by Ising models • Up to the second-order statistics are considered • Heavy computational complexity for parameter estimation

When $\sigma_i(t) = 0$ in Eq. (16), the solution is given by

$$V_i(t) = V_i(0)e^{-g_i t} + \sum_j \int_{-\infty}^{t} \exp(-g_i(t-s))I_{ij}(t)ds. \tag{19}$$

If we assume that $\kappa_{ij}(\cdot)$ is the Dirac's delta function and that t is much greater than $1/g_i$. Then, Eq. (19) can be approximated by

$$V_i(t) = \sum_j \sum_{\{f:t_j^{(f)}<t\}} \exp(-g_i(t - t_j^{(f)})). \tag{20}$$

By choosing $f(V) \propto \exp(-\beta(V - V_{th}))$ and discretizing the time so that $dt = 1$, the combination of Eqs. (20) and (18) reduces to the GLM (15) with $A_{i0} = -\beta V_{th}$, $A_{ij}(k) = \beta \exp(-g_i k)$, and exponential inverse link function $\phi(\cdot) = \exp(\cdot)$. For more detailed discussion, Gerstner & Kistler (2002), Gerstner et al. (2014), Paninski, Pillow, & Lewi (2007).

5.1.4. Network likelihood models

Network likelihood models (NLMs) (Kim et al., 2011; Okatan et al., 2005; Stevenson et al., 2009) are often adopted as a generative model for spike-train data in a continuous-time domain. Let $N_i(t)$ be the total number of the ith neuron's spikes observed before time t. In NLMs, it is assumed that $N_i(t)$ follows an inhomogeneous Poisson process $Poisson(\cdot|\lambda_i(t))$ with the conditional intensity function

$$\lambda_i(t) = \exp\left(A_{i0} + \sum_{j=1}^{P}\sum_{k=1}^{K} A_{ij}(k)I_{jk}(t)\right), \tag{21}$$

where

$$I_{jk}(t) = \int_0^t \xi_k(t-s)N_{j'}(s)ds \tag{22}$$

is a convolution of a linear filter $\xi_k(\cdot)$ and a spiking history of the jth neuron. A typical example of the linear filter is a rectangular window of duration W defined as

$$\xi_k(u) = \begin{cases} 1 & (\text{if } u \in [(k-1)W, kW)) \\ 0 & (\text{otherwise}). \end{cases} \tag{23}$$

NLMs can be converted into GLMs if the spiking history $N_i(t)$ is discretized into bins with a fixed window W, and W is so small that any bin has at most a single spike.

5.1.5. Calcium fluorescence model

When $x_i(t)$ is a continuous variable indicating the intensity of calcium fluorescence, we have to consider that the fluorescence signal has a fast initial rise upon an action potential followed by a slow decay. A standard model to reflect this feature is as follows (Mishchenko et al., 2011):

$$z_i(t+1) = (1-\alpha_i)z_i(t) + s_i(t) \tag{24}$$

$$x_i(t) = a_i z_i(t) + b_i + \zeta_i(t), \quad \zeta_i(t) \sim \mathcal{N}(0, \tau), \tag{25}$$

where $z_i(t)$ denotes the intracellular calcium concentration and $s_i(t)$ is a spike indicator variable such that $s_i(t) = 1$ if the ith neuron fires at time t and $s_i(t) = 0$ otherwise. $\theta = \{\alpha_i, a_i, b_i, \tau_i | i = 1, \ldots, P\}$ comprises the parameters of the model. Nonlinearities such as saturation can also be modeled as proposed by Vogelstein et al., (2009). In general, we cannot directly observe the variable $s_i(t)$ in this setting. To cope with this issue, Eqs. (24) and (25) are often combined with Eqs. (15a) and (15b) in which $x_i(t)$ is replaced by $s_i(t)$.

5.1.6. Hawkes process model

Linderman & Adams (2014, 2015) propose a Hawkes multivariate process to model a network of purely excitatory neurons. The model is considered as a generalized linear model (Section 5.1.2) with Poisson observations and a linear link function. The network model is defined by a binary matrix that indicates the existence of a directed connection between two neurons, a second weight matrix to represent the strength of each connection, and a vector specifying the transmission delay distribution for each directed connection.

Linderman & Adams (2015) enhanced the computational performance of their former approach (Linderman & Adams, 2014) with a new discrete time model that assumes that neurons do not interact faster than an arbitrary time unit and a variational approximation of the former Gibbs sampling solution in order to make the model fully conjugate.

5.1.7. Dynamic Bayesian Network

Dynamic Bayesian Networks (DBN) (Murphy, 2002) extend Bayesian Networks for time-series modeling. A DBN is usually defined as a directed acyclic graph where nodes represent random variables at particular times, and edges indicate a conditional probability dependence $P(x_{i,t}|x_{j,t-k})$ where $x_{i,t}$ denotes the ith neuron's activity at that time t.

Eldawlatly et al. (2010) demonstrated the feasibility of using DBM to infer the effective connectivity between spiking cortical neurons simulated with a generalized linear model (see Section 5.1.2). They use a simulated annealing algorithm to search the space of network structures and conditional probability parameters. Patnaik et al. (2011) present a significantly faster fitting algorithm that identifies, for each node, parent-sets with mutual information higher than a user-defined threshold. An upper bound of the Kullback–Leibler divergence between the inferred distribution and the true distribution is defined as a function of the user-defined threshold.

5.1.8. Maximum entropy model

The maximum-entropy model (Roudi et al., 2015; Yeh et al., 2010) assumes that the network state probability distribution is given by an exponential function of the network energy $E[S_i] = E[(x_1, \ldots, x_n)]$ such that entropy is maximized while satisfying any statistical constraints. When first and second-order statistics are given, the state probability distribution is given by

$$\begin{aligned} P(x_1, \ldots, x_n) &= \frac{1}{Z}\exp(-E[(x_1, \ldots, x_n)]) \\ &= \frac{1}{Z}\exp(\sum_i b_i x_i + \sum_{i \neq j} J_{ij} x_i x_j). \end{aligned} \tag{26}$$

This is an extension of the Ising model (McCoy, 2010) with spatial connections potentially occurring between any neurons as well as temporal correlations.

The main limitation of the maximum entropy model is its computational complexity. Recent studies demonstrated its applicability to a few tens of neurons using only first and second-order statistics without temporal correlations (Yeh et al., 2010).

5.2. Estimation of model parameters

5.2.1. Maximum likelihood method

The standard method to determine model parameters is the maximum likelihood (ML) method. The likelihood of a parameter vector θ given a data set D is defined as $p(D|\theta)$, the probability of reproducing the data. Here we denote the negative log-likelihood function as $J(\theta|D) = -\log p(D|\theta)$. In the ML method, parameters are chosen such that

$$\theta^* = \underset{\theta}{\operatorname{argmin}} J(\theta|D).$$

When the generative model uses a Gaussian distribution for observed data, the ML method reduces to *the least squares method.* For example, in the case of the AR model (12), maximization of the log likelihood is equivalent to minimization of *the sum of squared residuals*

$$\begin{aligned} J(\theta|D) &= \sum_{i=1}^{P}\sum_{t=1}^{T}\epsilon_i^2(t) \\ &= \sum_{i=1}^{P}\sum_{t=K+1}^{T}\left[x_i(t) - A_{i0} - \sum_{j=1}^{P}\sum_{k=1}^{K}A_{ij}(k)x_j(t-k)\right]^2, \end{aligned} \tag{27}$$

where $D \equiv \{x_i(t)|i = 1, \ldots, P;\ t = 1, \ldots, T\}$ denotes the observed data set.

This optimization can be achieved analytically in the case of least square problem, or in general by iterative optimization algorithms such as the gradient descent methods. When the model is represented using a set of hidden variables, a standard way is to use the expectation–maximization (EM) algorithms.

5.2.2. Regularization and Bayesian inference

A disadvantage of the ML method is that it often suffers from overfitting when the number of parameters is large relative to the amount of data. A common way to deal with this issue is to introduce regularization to the parameters. From a Bayesian statistical viewpoint, it assumes a prior distribution for the parameters. This makes explicit the assumption for connection inference, which is necessary due to the ill-posed nature of the inverse problem.

The objective function with a regularization term is given as

$$\theta^* = \underset{\theta}{\operatorname{argmin}} \{J(\theta|D) + \lambda\mathcal{R}(\theta)\},$$

where $\mathcal{R}(\cdot)$ is a non-negative function and λ is a constant that controls the strength of regularization. The most common regularizer is $L2$-norm regularizer, or the Ridge regularizer,

$$\mathcal{R}(\theta) = \sum_r \theta_r^2, \tag{28}$$

where r indexes the element of the set of parameters. In the Bayesian framework, this is equivalent to assuming a Gaussian prior distribution for the parameters. Another common regularizer is the $L1$-norm regularizer, or least absolute shrinkage and selection operator (LASSO) regularizer,

$$\mathcal{R}(\theta) = \sum_r |\theta_r|, \tag{29}$$

which favors a sparse solution with many parameters being zero. From a Bayesian viewpoint, this is equivalent to assuming a Laplace (exponential in absolute value) prior distribution.

Besides introducing regularization, Bayesian inference has several advantages over the ML method. For example, if the model has hidden variables, Bayesian inference is often used for estimating them as well as the model parameters (Mishchenko et al., 2011). Also, the reliability of each value in the parameter space can be evaluated as the posterior distribution. The high density region of the posterior distribution is called the Bayesian credible region, which can be used as an alternate to the confidence interval in the statistical test (Bowman, Caffo, Bassett, & Kilts, 2008). Another advantage is that the marginal likelihood, defined by the Bayes' theorem, can be used for a criterion to select the best of several possible models (Friston & Penny, 2011) (Section 2.5).

5.2.3. Approximate Bayesian inference methods

While Bayesian inference offers favorable features as above, exact computation for the posterior distribution and the marginal likelihood is often analytically intractable. Thus in practice it is important to select an approximation method. In the following, we briefly review approximation methods for the Bayesian inference. Details of their derivations and algorithms are beyond the scope of this paper and can be found in other articles (Chen, 2013; Murphy, 2012).

1. Monte Carlo Sampling approximates the target distribution (or value) as an aggregation (or average) of the finite number of random samples. Gibbs sampling (Casella & George, 1992), Metropolis–Hastings (Hastings, 1970) and sequential importance re/sampling (Liu & Chen, 1998) algorithms are typical examples of this class.
2. Laplace Approximation (Raftery, 1996) is a deterministic approximation applicable to cases in which the MAP estimator can be easily obtained. The central idea is to approximate the target distribution as a multivariate Gaussian distribution using the Hessian matrix (the second-order partial derivatives) of the logarithm of the posterior distribution; thus, the Laplace approximation is not suitable for cases in which the posterior distribution is multi-modal or asymmetric.
3. Variational Bayes (Attias, 1999) is another deterministic approximation method derived from the variational mean-field theory in statistical mechanics. Let us consider a case in which we want to obtain the posterior distribution $p(Z|D)$, where $Z = (z_1, \ldots, z_m)$ is a set of all unknown variables (i.e. hidden variables and model parameters) such that z_i $(i = 1, \ldots, m)$ is a partition of Z. Also, consider the probability distribution family of Z that can be factored as $q(Z) = \prod_{i=1}^{M} q(z_i)$. In the variational Bayes method, we approximate $p(Z|D)$ by optimizing $q(Z)$ to minimize the KL divergence between $q(Z)$ and $p(Z|D)$. Optimization is achieved by an algorithm similar to the expectation and maximization (EM) algorithm. Variational Bayes is suitable for cases in which the joint distribution $p(D, Z)$ is an instance of the exponential families (Wainwright & Jordan, 2007).

6. Case study

In this section, we review several examples of connectivity inference studies, from both model-free and model-based approaches. We focus on challenges addressed by each study at each stage of the data processing pipeline (Fig. 1).

6.1. Model-free approaches

The First Neural Connectomics Challenge (Guyon et al., 2014) encouraged development of very diverse solutions. Remarkably, the top three solutions were all model-free methods. The organizers provided simulated neural network data sets for training and testing, as well as key references about the problem and sample code to get started. Neural network data sets were simulated using leaky integrate-and-fire neurons with short term synaptic depression implemented in the NEST simulator and spike trains were transformed to fluorescence time-series using a fluorescence response model of calcium markers inside neurons. Each data set consisted of a one-hour time-series of neural activities obtained from fluorescence signals sampled at 20 ms intervals with values normalized in the interval [0, 1]. Organizers also provided information about the position of each neuron in an area of 1 mm^2 and inter-neuron connectivity labels (i.e. excitatory connection or no connection). A validation data set was provided for performance comparison by the Area Under the ROC Curve (AUC; see Section 2.5). Finally, the score on a separated test data set was used for the final ranking of teams.

The three best solutions and the baseline method provided by challenge organizers all consisted of several components: data pre-processing, main connectivity inference, and post-processing steps as discussed in Section 2 (Fig. 2). Below we review these top-ranked methods.

6.1.1. Partial-correlation and averaging

The first prize solution (Sutera et al., 2014) achieved a performance of 0.94161 (AUC score). Its pre-processing consisted of four steps: (i) low-pass filtering to remove noise, excessive fluctuations, and light scattering artifacts, (ii) backward differentiation for spike detection, (iii) hard thresholding to eliminate small values below a positive parameter τ, and (iv) weighting spike importance as a function of the inverse of network overall activity. The motivation for this last step was to eliminate effects of synchronized bursting periods, much as generalized transfer entropy does (see Section 4.2).

The main connectivity inference employed the Partial-Correlation (PC) matrix (Section 4.1), using the real valued signal computed in previous pre-processing steps. Post-processing consisted of two steps: (i) Several PC matrices were averaged according to different $\tau's$ and different low pass filters to increase the robustness of the solution. (ii) The symmetric average PC matrix was transformed into a directional indicator by multiplying each edge by an orientation weight computed according to the average activation delay between each neuron pair.

The main difficulty in scaling this solution to larger neural networks is the computation burden for calculating the inverse matrices. As an example, computation of the challenge solution connection matrix with 1000 neurons took 30 h on a 3 GHz i7 desktop PC with 7 GB of RAM.

6.1.2. Matrix deconvolution and adaptive averaging

The major features of the second prize solution (Magrans & Nowe, 2014) are that it used matrix deconvolution for eliminating indirect connections and introduced learning to optimally combine several connectivity matrices rather than just using simple averaging. The pre-processing pipeline consisted of three steps: (i) spike train inference based on the OOPSI algorithm (Vogelstein, 2009), (ii) hard thresholding according to a parameter value τ, as in the first prize solution, and (iii) removal of time segments with overall network activity above a given threshold θ.

Connectivity inference employed Pearson correlation between the real valued signal computed from pre-processing. A network deconvolution algorithm (Feizi et al., 2013) was then used to

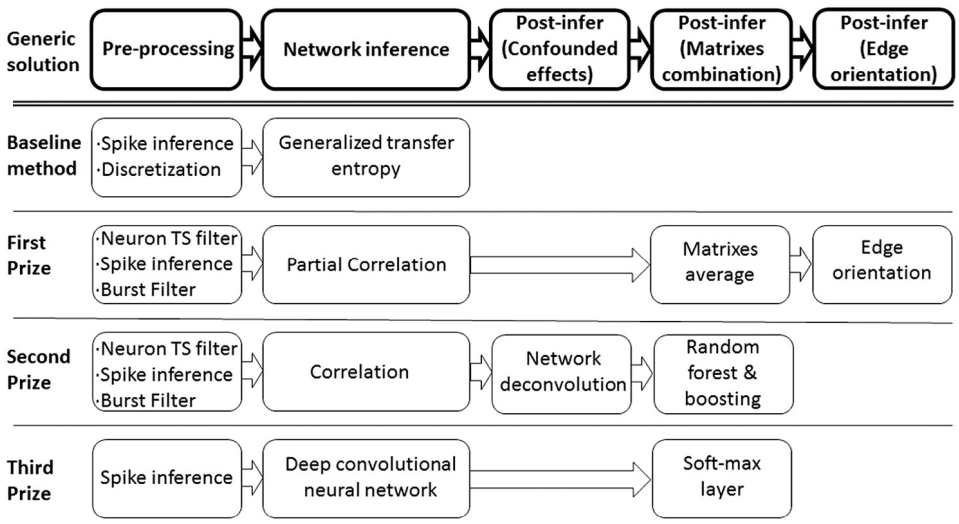

Fig. 2. Summary of top solutions of the First Neural Connectomics Challenge. The baseline method and the three winning methods are outlined according to their pre-processing, main connectivity inference, and post-processing steps. Note that not all methods implement all steps.

eliminate the combined effect of indirect paths. If the effect of direct connection is given by matrix W_d, under the assumption of linearity, combined effects of all direct and indirect connections follow

$$W_o = W_d + W_d^2 + W_d^3 + \cdots = W_d(I - W_d)^{-1}. \tag{30}$$

From this relationship, the matrix deconvolution method estimates the direct connection matrix W_d from the observed connections matrix W_o by

$$W_d = W_o(I + W_o)^{-1}. \tag{31}$$

Finally, connectivity matrices computed according to different values of τ and θ are combined, but unlike the first prize solution, using a function learned with a non-linear regression method for optimal performance.

Computation of the challenge solution took nearly 48 h on a 3 GHz i7 desktop PC with 32 GB of RAM. The most significant limitation of this solutions is its high computational cost. It does not try to infer self-connections. It does not try to identify the causal direction. It assumes that both training and testing networks have similar statistical properties.

6.1.3. Convolutional neural network approach

The third prize solution (Romaszko, 2014) proposed to automatically extract features from binary spike train pairs using a Convolutional Neural Network (CNN). Pre-processing consisted of three steps: (i) spike train inference using discrete differentiation, (ii) hard thresholding as in the first prize solution, and (iii) spike train normalization in [0,1]. Feature extraction was done with a CNN based on Lenet5 (LeCun, Bottou, Bengio, & Haffner, 1998) followed by a softmax layer that produced binary output in the event of a connection. This method was not designed to evaluate directions of connections.

Input data consisted of binary matrices of 3 by 330 where rows 1 and 2 corresponded to segments of the spike trains of two neurons. Row 3 contained information about the overall network activity, making it possible to identify synchronous bursting episodes. Network training was done with gradient descent.

The computational cost for this solution is very high. For instance, the challenge solution took more than 3 days on 8 server machines working in parallel, where each machine was equipped with 32 GB of RAM and GPU unit with 2496 cores. In addition to the extremely high computational cost, this solution has the same limitations as the second prize solution.

After the Connectomics Challenge, Veeriah et al. (2015) further advanced the CNN approach by integrating both the pre-processing step of spike train inference and connectivity inference into a single neural network architecture to surpass the first prize performance using the same data set. Its architecture consisted of two sub-networks and a final classification layer: (i) a convolutional neural network with max-pooling layers responsible for identifying relevant shapes in the fluorescence time-series with tolerance for minor time translations, (ii) a recurrent neural network (RNN) to model temporal sequences of relevant events. These are duplicated to capture the features of each neuron pair. Finally, a dynamically programmed layer aligned the RNN outputs and computed a connection probability for each neuron pair. Remarkably, this method does not require a separate pre-processing step to handle the synchronized bursting phenomenon.

Although the concept of an end-to-end artificial neural network is appealing, the performance comparison in Veeriah et al. (2015) deserves further consideration. Their reconstructed performances for generalized transfer entropy and partial correlation methods are lower than the performance documented during the First Neural Connectomics Challenge using the same data sets (Guyon et al., 2014; Orlandi et al., 2014; Sutera et al., 2014).

While these CNN-based approaches presented good performance with simulated data, it remains to be seen whether such classifiers generalize well to real data, for which ground truth training data are rarely available.

6.1.4. Other model-free approaches

Beyond the main results of the First Neural Connectomics Challenge, several *in vivo* and *in vitro* studies rely on model-free methods. Fujisawa et al. (2008) use silicon microelectrode arrays for *in vivo* recording from layers 2, 3 and 5 of the medial prefrontal cortex in rats during a working memory task. Connectivity inference is performed by identifying sharp spikes or troughs in the cross-correlograms. Connectivity significance is assessed by first creating several sets of slightly perturbed spike trains and then computing the statistical significance of the original cross-correlograms with respect to those constructed with the perturbed data.

Cohen & Kohn (2011) discuss a recent surge in cortical processing studies enabled by recording technologies like microelectrode arrays and calcium imaging (see Section 2.5.2). They summarize possible causes of discrepant findings in several correlation-based

studies due to technical reasons, i.e., poor spike sorting, experimental factors like different external stimuli, different time bins and/or spike train durations, or confounded effects due to non-stationary internal states. They suggest that multivariate point process models provide a more complete and statistically principled approach to cope with the challenges of inferring the connectivity structure.

6.2. Model-based approaches

6.2.1. Generalized linear models

Pillow and colleagues applied GLM frameworks for a stochastic integrate-and-fire neuron model (Paninski et al., 2004) to data of a complete neural recording from ganglion cells in a retina slice (Pillow et al., 2008). They constructed a model including both stimulus response and cross-connections of all neurons and showed through model-based analysis that correlated firing can provide additional sensory information.

Stevenson and colleagues derived a Bayesian inference framework for a spiking neuron model with arbitrary synaptic response kernels (Stevenson et al., 2009). They applied the method to neural recording data from monkey motor cortex and used the log likelihood and correlation coefficient criteria for cross validation. They further used infinite relational model clustering (Kemp, Tenenbaum, Griffiths, Yamada, & Ueda, 2006) to detect cluster structures among recorded neurons.

While Stevenson et al. (2009) used arbitrary synaptic kernel functions with discrete time bins, Song and colleagues (Song et al., 2013) proposed using a set of kernel functions, such as B-splines, with which smoothness of kernel functions is built-in with a relatively small number of parameters.

Oba et al. (2016) propose a GLM framework combined with empirical Bayesian testing. Null samples are created by time-shifting real spike trains for a sufficiently large time lag. They show improved computational performance without decreasing inference performance on a simulated neural network. They also apply this method to real calcium imaging data from a cultured slice of the CA3 region of rat hippocampus.

6.3. Calcium fluorescence model

In applying a connection estimation method to calcium fluorescent imaging data, a basic way is to estimate spike trains from fluorescence waveforms by spike deconvolution and then to apply a spike-based connectivity inference algorithm. Mishchenko et al. (2011) proposed a framework combining both steps of spike estimation and connection estimation into a unified stochastic generative model. Fletcher & Rangan (2014) proposed a computationally less expensive variant of this approach.

7. Discussion

7.1. Challenges and solutions

While model-free methods usually address pre- and post-processing separately from connectivity inference, model-based methods often address issues such as noise and connection directionality in the main inference process by incorporating those factors into generative models.

The distinction between apparent and real connections, as well as their directionality, is incorporated into neural dynamics equations in model-based methods. Weights most consistent with data are selected by the maximum likelihood or maximum posterior probability criterion. Among model-free methods, transfer entropy methods address connection directionality directly during the inference, while removal of apparent connections can be addressed by matrix deconvolution in post-processing (Magrans & Nowe, 2014). Partial-Correlation can also remove apparent connections but is not able to identify the causal direction. Sutera et al. (2014) propose a post-processing step to identify the causal direction. Temporal resolution of calcium imaging imposes severe performance limitations to these methods. Better solutions to identify the direction and to infer apparent connections should involve improving both algorithms and instrumentation. Table 3 summarizes solutions that were devised to overcome challenges along the data processing pipeline.

7.1.1. Non-stationarity

Modeling synaptic plasticity is a key to understand how memory and learning mechanisms are realized in neural circuits. Recent solutions to this challenge incorporate synaptic dynamics into a GLM framework and improved scalability within Bayesian (Linderman et al., 2014) and convex optimization settings (Stevenson & Koerding, 2011). Using a model-free approach to understand evolution of synaptic weights, Wollstadt et al. (2014) proposed a transfer entropy estimator that requires an ensemble of spike trains from equivalent and independent experiments.

Synaptic plasticity is not the sole source of non-stationarity. Time periods when a large percentage of neurons fire at a high rate is an additional non-stationary phenomenon and a source of confusion for most network inference methods. Generalized transfer entropy (Section 4.2.6), screens out the use of non-informative time periods. A similar selection could be developed for other model-free methods.

In Section 6.1 we also discussed how winning solutions of the First Neural Connectomics Challenge chose a modular approach with a dedicated pre-processing step to remove non-informative time periods before applying different connectivity indicators. We further discussed a deep neural network solution by Veeriah et al. (2015) that surprisingly, despite the lack of any pre-processing step or any specific design feature to remove high-rate time periods, is able to achieve improved performance with respect to the winning solution. A generalization of the above bi-modal switching behavior can also be accommodated with a model-based approach using a hidden Markov model (Linderman, Johnson, Datta, & Adams, 2015).

7.1.2. Architecture

Pre/post-processing methods have the potential to improve network reconstruction performance across different methods. For instance, modular architectures like the top solutions of the connectomics challenge (Section 6.1) implement a number of pre-processing steps to reduce noise and to infer spike trains. However, in applying such modular approaches, care has to be taken not to lose valuable information about the underlying direct connectivity and the directionality. On the other side of the spectrum, the approach using a deep neural network (Veeriah et al., 2015) is unique in providing solutions for multiple pre-processing and post-processing steps within a coherent model-free architecture.

In the model-based approach, Mishchenko et al. (2011) and later Fletcher & Rangan (2014) employed time-series of neural activities obtained from fluorescence signals as inputs, while spike times at an arbitrary sampling rate were additional latent variables. Table 3 summarizes solutions that were devised to overcome each of the challenges. We can observe that each solution was implemented either as a pre/pro-processing step or within the main inference method.

Table 3
Summary matrix of the solutions that were devised to overcome each of the challenges. We can observe that each solution was implemented either as a pre/pro-processing step or within the main inference method.

Challenges	Pre-processing	Connection inference		Post-processing
		Model-free	Model-based	
Apparent connection		Sutera et al. (2014) and Veeriah et al. (2015)	Pillow et al. (2008), Stevenson et al. (2009), Mishchenko et al. (2011) and Fletcher and Rangan (2014)	Magrans and Nowe (2014)
Directionality		Stetter et al. (2012), Garofalo et al. (2009), Ito et al. (2011) and Veeriah et al. (2015)	Pillow et al. (2008), Stevenson et al. (2009), Mishchenko et al. (2011) and Fletcher and Rangan (2014)	Sutera et al. (2014)
Cellular diversity				
Synaptic diversity			Pillow et al. (2008), Stevenson et al. (2009), Mishchenko et al. (2011) and Fletcher and Rangan (2014)	
Non-stationarity	Cohen and Kohn (2011), Sutera et al. (2014), Magrans and Nowe (2014) and Garofalo et al. (2009)	Wollstadt, Martínez-Zarzuela, Vicente, Díaz-Pernas, and Wibral (2014), Stetter et al. (2012) and Veeriah et al. (2015)	Linderman, Stock, and Adams (2014)	
Noise	Cohen and Kohn (2011), Sutera et al. (2014), Magrans and Nowe (2014), Wollstadt et al. (2014), Stetter et al. (2012) and Garofalo et al. (2009)	Veeriah et al. (2015)	Pillow et al. (2008), Stevenson et al. (2009), Mishchenko et al. (2011) and Fletcher and Rangan (2014)	
Time/Space resolution		Veeriah et al. (2015)	Mishchenko et al. (2011) and Fletcher and Rangan (2014)	
Hidden neuron/External input			Kulkarni and Paninski (2007), Vidne, Ahmadian, Shlens, Pillow, Kulkarni, Litke, Chichilnisky, Simoncelli, and Paninski (2012) and Rezende, Wierstra, and Gerstner (2011)	
Prior knowledge			Pillow et al. (2008), Stevenson et al. (2009), Mishchenko et al. (2011) and Fletcher and Rangan (2014)	
Scalability		Sutera et al. (2014) and Magrans and Nowe (2014)	Fletcher and Rangan (2014)	

7.1.3. Scalability

A major drawback to model-based methods is their scalability. The more sophisticated the model, the more parameters need to be estimated, which requires more data sampled from a stationary distribution. Prior knowledge, such as sparseness in connections, can be addressed in model-based methods by assuming a prior distribution in the model parameters and by applying Bayesian inference. Introduction of a sparseness prior, or an equivalent regularization term, can make inference from smaller samples more reliable, but this often increases the computational burden.

7.2. Hidden neurons

While neural recording methods are progressing rapidly, allowing whole-brain imaging with cellular resolution in small animals like *Caenorhabditis elegans* (Nguyen et al., 2016) and zebra fish (Ahrens et al., 2013), monitoring all neurons in the brain is still not possible. In typical calcium fluorescent imaging, neurons in only one section of a cortical column are recorded. Neglecting hidden neurons within the network, or unobservable external inputs, can infer erroneous connections. Methods for addressing this hidden input problem are still in early stages of development (Roudi et al., 2015).

The issue of hidden nodes, however, is not the only problem in neural connectivity inference. Similar problems have been addressed in gene regulation and signaling cascade networks, for example, and methods developed in other fields of computational biology and network science may provide helpful intuition and guidance (Su, Lai, Wang, & Do, 2014).

The challenge of hidden nodes groups different application scenarios under the same name, but the common denominator here is a generative model that consists of observed and hidden components. GLM (Section 5.1.2) and maximum entropy settings (Section 5.1.8) are the most common approaches to describe the observed neurons. However, the key differential contribution in all cases is the hidden neurons model. A single, latent process can model hidden inputs as random effects, enhancing network inference among observed neurons by avoiding false connections due to common hidden inputs (Kulkarni & Paninski, 2007; Vidne et al., 2012). A more sophisticated group of contributions proposes multiple latent processes, for instance to study the feasibility of biophysically plausible hypotheses about how multi-level neural circuits are able to learn and express complex sequences (Rezende et al., 2011). Switching behavior, described in the previous section, can also be seen as a special case of the hidden nodes challenge.

7.3. Incorporating prior knowledge

Detailed anatomical synaptic maps (Yook, Druckmann, & Kim, 2013), and connectivity maps between cell types across cortical layers (Potjans & Diesmann, 2014) are valuable sources of prior information that should be exploited to improve both inference and computational performance. A straightforward, model-based approach would be to exploit anatomical prior information using more sophisticated regularizers like the adaptive elastic net (Zou & Zhang, 2009), by embedding anatomical information in the adaptive weights instead of computing them using ordinary least squares (Wu et al., 2016). Prior information could also be incorporated as a post-processing method using graph sparsification algorithms to preserve certain graph theoretical properties (Ebbes, Huang, Rangaswamy, Thadakamalla, & Unit, 2008; Lindner, Staudt, Hamann, Meyerhenke, & Wagner, 2015).

A possible way to deal with hidden neurons when analyzing cortical microcircuits is to take advantage of the highly replicated

structure across layers and cortical columns. A possible framework to implement this idea, proposed by Kim and Leskovec (2011), infers parameters of a Kronecker model. In other words, a low-dimensional connectivity graph that approximately self-replicates across observed and the hidden parts. Within this application, exploitation of prior knowledge could enhance both computational and inferential performance.

The network inference problem could also be considered as a process of selecting a sub-set of pre-synaptic input neurons for each neuron. Therefore, it would be reasonable to explore application of feature selection algorithms (Liu & Motoda, 2012) to the problem at hand. From this point of view, multi-task feature selection algorithms (Obozinski, Taskar, & Jordan, 2006; Wang, Chang, Li, Sheng, & Chen, 2016; Zhou, Jin, & Hoi, 2010) may be another interesting way to take advantage of the highly replicated structure across layers and cortical columns. These algorithms propose clever ways to jointly learn features across several tasks, maximizing information sharing while minimizing negative transfer. Therefore, application of these methods has the potential to deliver superior inference and computational performance with respect to single-task learning approaches while using the same amount of data.

A common assumption of many inference methods is a simplistic model structure that does not represent the true synaptic and cellular diversity of local neural microcircuits (see Section 3.1). Future research methods should aim for approaches able to fit more biophysically plausible models. Recent wide-field calcium imaging of thousands of neurons over millimeters of brain tissue (Mohammed, Gritton, Tseng, Bucklin, Yao, & Han, 2016), the large number of latent parameters to model hidden neurons and non-stationarity, are all sources of increasing computational complexity and a strong impetus to continue improving the computational efficiency of network inference methods (Lee, Lim, & Ong, 2016).

8. Conclusion

In this paper, we reviewed methods for inference of neural connectivity based on activity recordings from a large number of neurons. We first identified biophysical and technical challenges along the data processing pipeline and then formulated model-free and model-based approaches for the core process of connectivity inference. We further investigated how previous work addressed those challenges using various methods. As a result, we identified favorable methods that deserve further technical developments, most notably coping with hidden neurons.

Connectivity inference itself is an interesting and deep mathematical problem, but the goal of connectivity inference is not only to precisely estimate the connection weight matrix, but also to illustrate how neural circuits realize specific functions, such as sensory inference, motor control, and decision making, and to understand baseline brain dynamics, upon which those function would be based. If we can perfectly estimate network connections from anatomical and activity data, then computer simulation of the network model should be able to reproduce network function as well as resting-state dynamics. But given inevitable uncertainties in connectivity inference, reconstruction of functions in a purely data-driven way might be difficult. How to extract or infer a functional or computational network from a data-driven network, or even to combine known functional constraints as a prior for connectivity inference, is a possible direction of future research.

Acknowledgments

This research was supported by the program for Brain Mapping by Integrated Neurotechnologies for Disease Studies (Brain/MINDS) from Japan Agency for Medical Research and development (AMED) under the Grant Number JP17dm0207030, KAKENHI Grant 16H06563 from Ministry of Education, Culture, Sports, Science and Technology (MEXT), and internal funding from the Okinawa Institute of Science and Technology Graduate University. We thank Steven D. Aird for editing the manuscript.

References

Aertsen, A., Gerstein, G., Habib, M., & Palm, G. (1989). Dynamics of neuronal firing correlation: modulation of "effective connectivity". *Journal of Neurophysiology*, *61*(5), 900–917.

Aho, K., Derryberry, D., & Peterson, T. (2014). Model selection for ecologists: the worldviews of AIC and BIC. *Ecology*, *95*(3), 631–636.

Ahrens, M. B., Li, J. M., Orger, M. B., Robson, D. N., Schier, A. F., Engert, F., et al. (2012). Brain-wide neuronal dynamics during motor adaptation in zebrafish. *Nature*, *485*(7399), 471–477.

Ahrens, M. B., Orger, M. B., Robson, D. N., Li, J. M., & Keller, P. J. (2013). Whole-brain functional imaging at cellular resolution using light-sheet microscopy. *Nature Methods*, *10*(5), 413–420.

Amunts, K., Ebell, C., Muller, J., Telefont, M., Knoll, A., & Lippert, T. (2016). The human brain project: Creating a european research infrastructure to decode the human brain. *Neuron*, *92*(3), 574–581. URL http://www.sciencedirect.com/science/article/pii/S0896627316307966.

Ask, M., & Reza, M. (2016). Computational models in neuroscience: How real are they? A critical review of status and suggestions. *Austin Neurology & Neurosciences*, *1*(2), 1008.

Attias, H. (1999). A variational Bayesian framework for graphical models. *Advances in Neural Information Processing Systems (NIPS)*, 209–215.

Barnett, L., Barrett, A. B., & Seth, A. K. (2009). Granger causality and transfer entropy are equivalent for Gaussian variables. *Physical Review Letters*, *103*(23), 238701.

Barzel, B., & Barabási, A.-L. (2013). Network link prediction by global silencing of indirect correlations. *Nature biotechnology*, *31*(8), 720–725.

Bekkers, J. M. (2009). Synaptic transmission: excitatory autapses find a function? *Current Biology*, *19*(7), R296–8.

Bonifazi, P., Goldin, M., Picardo, M. A., Jorquera, I., Cattani, A., Bianconi, G., et al. (2009). Gabaergic hub neurons orchestrate synchrony in developing hippocampal networks. *Science*, *326*(5958), 1419–1424.

Bowman, F. D., Caffo, B., Bassett, S. S., & Kilts, C. (2008). A Bayesian hierarchical framework for spatial modeling of fMRI data. *NeuroImage*, *39*(1), 146–156.

Brette, R., & Destexhe, A. (2012). Intracellular recording. In *Handbook of neural activity measurement*. Cambridge University Press.

Bullmore, E., & Sporns, O. (2009). Complex brain networks: graph theoretical analysis of structural and functional systems. *Nature Reviews Neuroscience*, *10*(3), 186–198.

Buzsaki, G. (2004). Large-scale recording of neuronal ensembles. *Nature Neuroscience*, *7*(5), 446–451. URL https://www.ncbi.nlm.nih.gov/pubmed/15114356, http://www.nature.com/neuro/journal/v7/n5/pdf/nn1233.pdf.

Casella, G., & George, E. I. (1992). Explaining the Gibbs sampler. *The American Statistician*, *46*(3), 167–174.

Chen, Z. (2013). An overview of Bayesian methods for neural spike train analysis. *Computational Intelligence and Neuroscience*, *2013*, 1.

Chiappalone, M., Vato, A., Berdondini, L., Koudelka-Hep, M., & Martinoia, S. (2007). Network dynamics and synchronous activity in cultured cortical neurons. *International Journal of Neural Systems*, *17*(02), 87–103.

Churchland, P. S., & Sejnowski, T. J. (1992). *The computational brain*. MIT Press.

Cohen, M. R., & Kohn, A. (2011). Measuring and interpreting neuronal correlations. *Nature Neuroscience*, *14*(7), 811–819.

Czarnecki, W. M., & Jozefowicz, R. (2014). Neural connectivity reconstruction from calcium imaging signal using random forest with topological features. In *ECML workshop - "Neural connectomics: From imaging to connectivity"*. Nancy, France.

Destexhe, A., & Bedard, C. (2013). Local field potential. *Scholarpedia*, *8*(8), 10713. Revision number 135811.

Dombeck, D. A., Graziano, M. S., & Tank, D. W. (2009). Functional clustering of neurons in motor cortex determined by cellular resolution imaging in awake behaving mice. *Journal of Neuroscience*, *29*(44), 13751–13760. URL http://www.ncbi.nlm.nih.gov/pubmed/19889987.

Ebbes, P., Huang, Z., Rangaswamy, A., Thadakamalla, H. P., & Unit, O. (2008). Sampling large-scale social networks: Insights from simulated networks. In *18th annual workshop on information technologies and systems*. Paris, France: Citeseer.

Eldawlatly, S., Zhou, Y., Jin, R., & Oweiss, K. G. (2010). On the use of dynamic bayesian networks in reconstructing functional neuronal networks from spike train ensembles. *Neural Computation*, *22*(1), 158–189.

Feizi, S., Marbach, D., Médard, M., & Kellis, M. (2013). Network deconvolution as a general method to distinguish direct dependencies in networks. *Nature biotechnology*, *31*(8), 726–733.

Fletcher, A. K., & Rangan, S. (2014). Scalable inference for neuronal connectivity from calcium imaging. In *Advances in neural information processing systems* (Vol. 27) (pp. 2843–2851).

Franaszczuk, P. J., Blinowska, K. J., & Kowalczyk, M. (1985). The application of parametric multichannel spectral estimates in the study of electrical brain activity. *Biological Cybernetics*, *51*(4), 239–247.

Friston, K. J. (2011). Functional and effective connectivity: a review. *Brain Connectivity*, *1*(1), 13–36.

Friston, K., & Penny, W. (2011). Post hoc Bayesian model selection. *NeuroImage*, *56*(4), 2089–2099.

Fujisawa, S., Amarasingham, A., Harrison, M. T., & Buzsáki, G. (2008). Behavior-dependent short-term assembly dynamics in the medial prefrontal cortex. *Nature Neuroscience*, *11*(7), 823–833.

Fujishiro, A., Kaneko, H., Kawashima, T., Ishida, M., & Kawano, T. (2014). In vivo neuronal action potential recordings via three-dimensional microscale needle-electrode arrays. *Scientific Reports*, *4*, 4868. URL http://www.ncbi.nlm.nih.gov/pubmed/24785307.

Garofalo, M., Nieus, T., Massobrio, P., & Martinoia, S. (2009). Evaluation of the performance of information theory-based methods and cross-correlation to estimate the functional connectivity in cortical networks. *PloS One*, *4*(8), e6482.

Gerstner, W., & Kistler, W. M. (2002). *Spiking neuron models: Single neurons, populations, plasticity*. Cambridge University Press.

Gerstner, W., Kistler, W. M., Naud, R., & Paninski, L. (2014). *Neuronal dynamics: From single neurons to networks and models of cognition*. Cambridge, UK: Cambridge Universty Press.

Gerwinn, S., Macke, J. H., & Bethge, M. (2010). Bayesian inference for generalized linear models for spiking neurons. *Frontiers in Computational Neuroscience*, *4*.

Guyon, I., Battaglia, D., Guyon, A., Lemaire, V., Orlandi, J. G., Ray, B., et al. (2014). Design of the first neuronal connectomics challenge: From imaging to connectivity. In *Neural networks, 2014 international joint conference on* (pp. 2600–2607). IEEE.

Harrison, L., Penny, W. D., & Friston, K. (2003). Multivariate autoregressive modeling of fMRI time series. *NeuroImage*, *19*(4), 1477–1491.

Hastings, W. K. (1970). Monte Carlo sampling methods using Markov chains and their applications. *Biometrika*, *57*(1), 97–109.

Hu, Y., Brunton, S. L., Cain, N., Mihalas, S., Kutz, J. N., & Shea-Brown, E. (2016). Feedback through graph motifs relates structure and function in complex networks. ArXiv preprint arXiv:1605.09073.

Insel, T. R., Landis, S. C., & Collins, F. S. (2013). The NIH brain initiative. *Science*, *340*(6133), 687–688.

Isomura, T., Ogawa, Y., Kotani, K., & Jimbo, Y. (2015). Accurate connection strength estimation based on variational bayes for detecting synaptic plasticity. *Neural Computation*, *27*(4), 819–844.

Ito, S., Hansen, M. E., Heiland, R., Lumsdaine, A., Litke, A. M., & Beggs, J. M. (2011). Extending transfer entropy improves identification of effective connectivity in a spiking cortical network model. *PloS One*, *6*(11), e27431.

Jog, M., Connolly, C., Kubota, Y., Iyengar, D., Garrido, L., Harlan, R., et al. (2002). Tetrode technology: advances in implantable hardware, neuroimaging, and data analysis techniques. *Journal of Neuroscience Methods*, *117*, 141–152.

Kandel, E. R., Schwartz, J. H., Jessell, T. M., et al. (2000a). Principles of neural science. In *The cells of the nervous system* (Vol. 4). New York: McGraw-Hill.

Kandel, E. R., Schwartz, J. H., Jessell, T. M., et al. (2000b). Principles of neural science. In *Overview of synaptic transmission* (Vol. 4). New York: McGraw-Hill.

Kemp, C., Tenenbaum, J. B., Griffiths, T. L., Yamada, T., & Ueda, N. (2006). Learning systems of concepts with an infinite relational model. In *AAAI* (Vol. 3) (p. 5.

Kim, M., & Leskovec, J. (2011). The network completion problem: Inferring missing nodes and edges in networks. In *SDM* (Vol. 11) (pp. 47–58). SIAM.

Kim, S., Putrino, D., Ghosh, S., & Brown, E. N. (2011). A granger causality measure for point process models of ensemble neural spiking activity. *PLoS Computational Biology*, *7*(3), e1001110.

Knox, C. K. (1981). Detection of neuronal interactions using correlation analysis. *Trends in Neurosciences*, *4*, 222–225.

Koyama, S., & Paninski, L. (2010). Efficient computation of the maximum a posteriori path and parameter estimation in integrate-and-fire and more general state-space models. *Journal of Computational Neuroscience*, *29*(1–2), 89–105.

Kulkarni, J. E., & Paninski, L. (2007). Common-input models for multiple neural spike-train data. *Network: Computation in Neural Systems*, *18*(4), 375–407.

Lang, E. W., Tomé, A., Keck, I. R., Górriz-Sáez, J., & Puntonet, C. (2012). Brain connectivity analysis: a short survey. *Computational Intelligence and Neuroscience*, *2012*, 8.

LeCun, Y., Bottou, L., Bengio, Y., & Haffner, P. (1998). Gradient-based learning applied to document recognition. *Proceedings of the IEEE*, *86*(11), 2278–2324.

Lee, Y., Lim, K. W., & Ong, C. S. (2016). Hawkes processes with stochastic excitations. In *Proceedings of the 33rd international conference on machine learning* (pp. 79–88).

Linderman, S. W., & Adams, R. P. (2014). Discovering latent network structure in point process data. In *ICML* (pp. 1413–1421).

Linderman, S. W., & Adams, R. P. (2015). Scalable Bayesian inference for excitatory point process networks. ArXiv preprint arXiv:1507.03228.

Linderman, S. W., Johnson, M. J., Datta, S. R., & Adams, R. P. (2015). Discovering switching autoregressive dynamics in neural spike train recordings. In *Computational and systems neuroscience (Cosyne)*.

Linderman, S., Stock, C. H., & Adams, R. P. (2014). A framework for studying synaptic plasticity with neural spike train data. In *Advances in neural information processing systems* (pp. 2330–2338).

Lindner, G., Staudt, C. L., Hamann, M., Meyerhenke, H., & Wagner, D. (2015). Structure-preserving sparsification of social networks. In *Proceedings of the 2015 IEEE/ACM International conference on advances in social networks analysis and mining 2015* (pp. 448–454). ACM.

Liu, H., & Motoda, H. (2012). *Feature selection for knowledge discovery and data mining* (Vol. 454). Springer Science & Business Media.

Liu, J. S., & Chen, R. (1998). Sequential Monte Carlo methods for dynamic systems. *Journal of the American Statistical Association*, *93*(443), 1032–1044.

Lizier, J. T. (2014). JIDT: an information-theoretic toolkit for studying the dynamics of complex systems. ArXiv preprint arXiv:1408.3270.

Lizier, J. T., Heinzle, J., Horstmann, A., Haynes, J.-D., & Prokopenko, M. (2011). Multivariate information-theoretic measures reveal directed information structure and task relevant changes in fMRI connectivity. *Journal of Computational Neuroscience*, *30*(1), 85–107.

Looger, L. L., & Griesbeck, O. (2011). Genetically encoded neural activity indicators. *Current Opinion in Neurobiology*, *22*, 18–23.

Lütcke, H., & Helmchen, F. (2011). Two-photon imaging and analysis of neural network dynamics. *Reports on Progress in Physics*, *74*(8), 086602.

Magrans, I., & Nowe, A. (2014). Supervised neural network structure recovery. In *ECML workshop -"neural connectomics: from imaging to connectivity"*. Nancy, France.

Mahmud, M., Pulizzi, R., Vasilaki, E., & Giugliano, M. (2015). Qspike tools: a generic framework for parallel batch preprocessing of extracellular neuronal signals recorded by substrate microelectrode arrays. *Recent Advances and the Future Generation of Neuroinformatics Infrastructure*, 248.

Markram, H. (2012). The human brain project. *Scientific American*, *306*(6), 50–55.

Martin, C. L., & Chun, M. (2016). The {BRAIN} initiative: Building, strengthening, and sustaining. *Neuron*, *92*(3), 570–573. URL http://www.sciencedirect.com/science/article/pii/S0896627316307899.

McCoy, B. (2010). Ising model: exact results. *Scholarpedia*, *5*(7), 10313. Revision number 123804.

Mishchenko, Y., Vogelstein, J. T., & Paninski, L. (2011). A Bayesian approach for inferring neuronal connectivity from calcium fluorescent imaging data. *Annals of Applied Statistics*, *5*(2B), 1229–1261.

Mohammed, A. I., Gritton, H. J., Tseng, H.-a., Bucklin, M. E., Yao, Z., & Han, X. (2016). An integrative approach for analyzing hundreds of neurons in task performing mice using wide-field calcium imaging. *Scientific Reports*, *6*.

Murphy, K. P. (2002). Dynamic bayesian networks. *Probabilistic Graphical Models, M. Jordan*, *7*.

Murphy, K. P. (2012). *Machine learning: a probabilistic perspective*. MIT Press.

Nguyen, J. P., Shipley, F. B., Linder, A. N., Plummer, G. S., Liu, M., Setru, S. U., et al. (2016). Whole-brain calcium imaging with cellular resolution in freely behaving caenorhabditis elegans. *Proceedings of the National Academy of Sciences*, *113*(8), E1074–E1081.

Oba, S., Nakae, K., Ikegaya, Y., Aki, S., Yoshimoto, J., & Ishii, S. (2016). Empirical Bayesian significance measure of neuronal spike response. *BMC Neuroscience*, *17*(1), 1.

Obozinski, G., Taskar, B., & Jordan, M. (2006). *Multi-task feature selection, Tech. rep. 2*. Statistics Department, UC Berkeley.

Okano, H., & Mitra, P. (2015). Brain-mapping projects using the common marmoset. *Neuroscience Research*, *93*, 3–7. URL http://www.ncbi.nlm.nih.gov/pubmed/25264372.

Okano, H., Sasaki, E., Yamamori, T., Iriki, A., Shimogori, T., Yamaguchi, Y., et al. (2016). Brain/minds: A japanese national brain project for marmoset neuroscience. *Neuron*, *92*(3), 582–590. URL http://www.sciencedirect.com/science/article/pii/S089662731630719X.

Okatan, M., Wilson, M. A., & Brown, E. N. (2005). Analyzing functional connectivity using a network likelihood model of ensemble neural spiking activity. *Neural Computation*, *17*(9), 1927–1961.

Orlandi, J. G., Ray, B., Battaglia, D., Guyon, I., Lemaire, V., & Saeed, M. (2014). First connectomics challenge: From imaging to connectivity. In *ECML workshop - "Neural connectomics: From imaging to connectivity"*. Nancy, France.

Orlandi, J. G., Stetter, O., Soriano, J., Geisel, T., & Battaglia, D. (2014). Transfer entropy reconstruction and labeling of neuronal connections from simulated calcium imaging. *PloS One*, *9*(6), e98842.

Paninski, L., Pillow, J., & Lewi, J. (2007). Statistical models for neural encoding, decoding, and optimal stimulus design. In T. D. Paul Cisek, & J. F. Kalaska (Eds.), *Progress in brain research: Vol. 165. Computational neuroscience: Theoretical insights into brain function* (pp. 493–507). Elsevier, URL http://www.sciencedirect.com/science/article/pii/S0079612306650310.

Paninski, L., Pillow, J. W., & Simoncelli, E. P. (2004). Maximum likelihood estimation of a stochastic integrate-and-fire neural encoding model. *Neural Computation*, *16*(12), 2533–2561.

Patnaik, D., Laxman, S., & Ramakrishnan, N. (2011). Discovering excitatory relationships using dynamic bayesian networks. *Knowledge and Information Systems*, *29*(2), 273–303.

Pillow, J. W., Paninski, L., Uzzell, V. J., Simoncelli, E. P., & Chichilnisky, E. (2005). Prediction and decoding of retinal ganglion cell responses with a probabilistic spiking model. *The Journal of Neuroscience*, *25*(47), 11003–11013.

Pillow, J. W., Shlens, J., Paninski, L., Sher, A., Litke, A. M., Chichilnisky, E. J., et al. (2008). Spatio-temporal correlations and visual signalling in a complete neuronal population. *Nature*, *454*(7207), 995–999. URL http://www.ncbi.nlm.nih.gov/pubmed/18650810.

Pnevmatikakis, E. A., Soudry, D., Gao, Y., Machado, T. A., Merel, J., Pfau, D., et al. (2016). Simultaneous denoising, deconvolution, and demixing of calcium imaging data. *Neuron*, *89*, 285–299.

Potjans, T. C., & Diesmann, M. (2014). The cell-type specific cortical microcircuit: relating structure and activity in a full-scale spiking network model. *Cerebral Cortex*, *24*(3), 785–806.

Raftery, A. E. (1996). Approximate Bayes factors and accounting for model uncertainty in generalised linear models. *Biometrika*, *83*(2), 251–266.

Rezende, D. J., Wierstra, D., & Gerstner, W. (2011). Variational learning for recurrent spiking networks. In *Advances in neural information processing systems* (pp. 136–144).

Romaszko, L. (2014). Signal correlation prediction using convolutional neural networks. In *ECML workshop - "Neural connectomics: From imaging to connectivity"*. Nancy, France.

Roudi, Y., Dunn, B., & Hertz, J. (2015). Multi-neuronal activity and functional connectivity in cell assemblies. *Current Opinion in Neurobiology*, *32*, 38–44.

Schreiber, T. (2000). Measuring information transfer. *Physical Review Letters*, *85*(2), 461.

Schrynemackers, M., Küffner, R., & Geurts, P. (2013). On protocols and measures for the validation of supervised methods for the inference of biological networks. *Frontiers in Genetics*, *4*.

Shannon, I. C. (1948). A mathematical theori of cornm unifications. *Bell System Technical Journal*.

Shimono, M., & Beggs, J. M. (2014). Functional clusters, hubs, and communities in the cortical microconnectome. *Cerebral Cortex*, bhu252.

Smith, A. C., Fall, C. P., & Sornborger, A. T. (2011). Near-real-time connectivity estimation for multivariate neural data. In *Engineering in medicine and biology society, EMBC, 2011 annual international conference of the IEEE* (pp. 4721–4724).

Sohn, Y., Choi, M.-K., Ahn, Y.-Y., Lee, J., & Jeong, J. (2011). Topological cluster analysis reveals the systemic organization of the Caenorhabditis elegans connectome. *PLoS Computational Biology*, *7*(5), e1001139.

Song, D., Wang, H., Tu, C., Marmarelis, V., Hampson, R., Deadwyler, S., et al. (2013). Identification of sparse neural functional connectivity using penalized likelihood estimation and basis functions. *Journal of Computational Neuroscience*, *35*(3), 335–357.

Sporns, O. (2012). *Discovering the human connectome*. MIT press.

Sporns, O. (2013). The human connectome: origins and challenges. *Neuroimage*, *80*, 53–61.

Sporns, O., Tononi, G., & Kötter, R. (2005). The human connectome: a structural description of the human brain. *PLoS Computational Biology*, *1*(4), e42.

Stetter, O., Battaglia, D., Soriano, J., & Geisel, T. (2012). Model-free reconstruction of excitatory neuronal connectivity from calcium imaging signals. *PLoS Computational Biology*, *8*(8), e1002653.

Stevenson, I., & Koerding, K. (2011). Inferring spike-timing-dependent plasticity from spike train data. In *Advances in neural information processing systems* (pp. 2582–2590).

Stevenson, I. H., Rebesco, J. M., Hatsopoulos, N. G., Haga, Z., Miller, L. E., & Kording, K. P. (2009). Bayesian inference of functional connectivity and network structure from spikes. *IEEE Transactions on Neural Systems Rehabilitation Engineering*, *17*(3), 203–213.

Su, R. Q., Lai, Y. C., Wang, X., & Do, Y. (2014). Uncovering hidden nodes in complex networks in the presence of noise. *Scientific Reports*, *4*, 3944. URL http://www.ncbi.nlm.nih.gov/pubmed/24487720.

Sutera, A., Joly, A., François-Lavet, V., Qiu, Z. A., Louppe, G., & Ernst, D. (2014). Simple connectome inference from partial correlation statistics in calcium imaging. In *ECML workshop - "Neural connectomics: From imaging to connectivity"*. Nancy, France.

Tateno, T., & Jimbo, Y. (1999). Activity-dependent enhancement in the reliability of correlated spike timings in cultured cortical neurons. *Biological Cybernetics*, *80*(1), 45–55.

Tkacik, G., Mora, T., Marre, O., Amodei, D., Berry, I., & Michael, J. (2014). Thermodynamics for a network of neurons: Signatures of criticality. ArXiv preprint arXiv:1407.5946.

Valdes-Sosa, P. A., Roebroeck, A., Daunizeau, J., & Friston, K. (2011). Effective connectivity: influence, causality and biophysical modeling. *Neuroimage*, *58*(2), 339–361.

Valdés-Sosa, P. A., Sánchez-Bornot, J. M., Lage-Castellanos, A., Vega-Hernández, M., Bosch-Bayard, J., Melie-García, L., et al. (2005). Estimating brain functional connectivity with sparse multivariate autoregression. *Philosophical Transactions of the Royal Society Series B (Biological Sciences)*, *360*(1457), 969–981.

Van Drongelen, W. (2006). *Signal processing for neuroscientists: an introduction to the analysis of physiological signals*. Academic Press.

Veeriah, V., Durvasula, R., & Qi, G.-J. (2015). Deep learning architecture with dynamically programmed layers for brain connectome prediction. In *Proceedings of the 21th ACM SIGKDD international conference on knowledge discovery and data mining* (pp. 1205–1214). ACM.

Vidne, M., Ahmadian, Y., Shlens, J., Pillow, J. W., Kulkarni, J., Litke, A. M., et al. (2012). Modeling the impact of common noise inputs on the network activity of retinal ganglion cells. *Journal of Computational Neuroscience*, *33*(1), 97–121.

Vogelstein, J. T. (2009). *OOPSI: A family of optimal optical spike inference algorithms for inferring neural connectivity from population calcium imaging*. The Johns Hopkins University.

Vogelstein, J. T., Watson, B. O., Packer, A. M., Yuste, R., Jedynak, B., & Paninski, L. (2009). Spike inference from calcium imaging using sequential Monte Carlo methods. *Biophysical Journal*, *97*(2), 636–655.

Wainwright, M. J., & Jordan, M. I. (2007). Graphical models, exponential families, and variational inference. *Foundations and Trends in Machine Learning*, *1*(1–2), 1–305.

Wang, S., Chang, X., Li, X., Sheng, Q. Z., & Chen, W. (2016). Multi-task support vector machines for feature selection with shared knowledge discovery. *Signal Processing*, *120*, 746–753.

White, J., Southgate, E., Thomson, J., & Brenner, S. (1986). The structure of the nervous system of the nematode Caenorhabditis elegans: the mind of a worm. *Philosophical Transactions of the Royal Society of London*, *314*, 1–340.

Wollstadt, P., Martínez-Zarzuela, M., Vicente, R., Díaz-Pernas, F. J., & Wibral, M. (2014). Efficient transfer entropy analysis of non-stationary neural time series. *PloS One*, *9*(7), e102833.

Wu, M.-Y., Zhang, X.-F., Dai, D.-Q., Ou-Yang, L., Zhu, Y., & Yan, H. (2016). Regularized logistic regression with network-based pairwise interaction for biomarker identification in breast cancer. *BMC Bioinformatics*, *17*(1), 1.

Yang, H. H., & St-Pierre, F. (2016). Genetically encoded voltage indicators: opportunities and challenges. *Journal of Neuroscience*, *36*(39), 9977–9989. URL https://www.ncbi.nlm.nih.gov/pubmed/27683896.

Yeh, F.-C., Tang, A., Hobbs, J. P., Hottowy, P., Dabrowski, W., Sher, A., et al. (2010). Maximum entropy approaches to living neural networks. *Entropy*, *12*(1), 89–106.

Yook, C., Druckmann, S., & Kim, J. (2013). Mapping mammalian synaptic connectivity. *Cellular and Molecular Life Sciences*, *70*(24), 4747–4757.

Yu, S., Huang, D., Singer, W., & Nikolić, D. (2008). A small world of neuronal synchrony. *Cerebral Cortex*, *18*(12), 2891–2901.

Zhou, Y., Jin, R., & Hoi, S. C. (2010). Exclusive lasso for multi-task feature selection. In *AISTATS* (Vol. 9) (pp. 988–995).

Ziv, Y., Burns, L. D., Cocker, E. D., Hamel, E. O., Ghosh, K. K., Kitch, L. J., et al. (2013). Long-term dynamics of ca1 hippocampal place codes. *Nature Neuroscience*, *16*(3), 264–266. URL http://www.ncbi.nlm.nih.gov/pubmed/23396101.

Zou, H., & Zhang, H. H. (2009). On the adaptive elastic-net with a diverging number of parameters. *Annals of Statistics*, *37*(4), 1733.